1981

Application of quasi-lagrangian diagnostics and FGGE data in a study of east-coast cyclogenesis.

Roman, Donald A.

Monterey, California. Naval Postgraduate School

NAVAL POSTGRADUATE SCHOOL
Monterey, California

THESIS

APPLICATION OF QUASI-LAGRANGIAN DIAGNOSTICS AND FGGE DATA IN A STUDY OF EAST-COAST CYCLOGENESIS

by

Donald A. Roman

September 1981

Thesis Advisor: Dr. Carlyle H. Wash

Approved for public release, distribution unlimited

SECURITY CLASSIFICATION OF THIS PAGE (When Data Entered)

REPORT DOCUMENTATION PAGE

READ INSTRUCTIONS BEFORE COMPLETING FORM

1. REPORT NUMBER	2. GOVT ACCESSION NO.
3. RECIPIENT'S CATALOG NUMBER	
4. TITLE (and Subtitle) Application of Quasi-Lagrangian Diagnostics and FGGE Data in a Study East-Coast Cyclogenesis	5. TYPE OF REPORT & PERIOD COVERED Master's Thesis September 1981
6. PERFORMING ORG. REPORT NUMBER	
7. AUTHOR(s) Donald A. Roman	8. CONTRACT OR GRANT NUMBER(s)
9. PERFORMING ORGANIZATION NAME AND ADDRESS Naval Postgraduate School Monterey, California 93940	10. PROGRAM ELEMENT, PROJECT, TASK AREA & WORK UNIT NUMBERS
11. CONTROLLING OFFICE NAME AND ADDRESS Naval Postgraduate School Monterey, California 93940	12. REPORT DATE September 1981
	13. NUMBER OF PAGES 89
14. MONITORING AGENCY NAME & ADDRESS(if different from Controlling Office)	15. SECURITY CLASS. (of this report)
	15a. DECLASSIFICATION/DOWNGRADING SCHEDULE

16. DISTRIBUTION STATEMENT (of this Report)

Approved for public release, distribution unlimited

17. DISTRIBUTION STATEMENT (of the abstract entered in Block 20, if different from Report)

18. SUPPLEMENTARY NOTES

19. KEY WORDS (Continue on reverse side if necessary and identify by block number)

East-Coast Cyclogenesis, Mass Budget, Quasi-Lagrangian Diagnostics, Cyclogenesis, Oceanic Storm, FGGE, Presidents' Day Storm, Stability Analysis, Synoptic Study

20. ABSTRACT (Continue on reverse side if necessary and identify by block number)

This synoptic study of an explosive deepening event, the Presidents' Day Storm of 17-20 February 1979, introduces and examines the Level III-b FGGE data of an oceanic storm. It applies the quantitative quasi-Lagrangian diagnostics techniques to both the FGGE data for a 48 hour period and a 24 hour LFM II prediction. Using a mass budget analysis in isobaric coordinates, the mass structure and circulation intensity are examined and

DD FORM 1 JAN 73 1473 EDITION OF 1 NOV 68 IS OBSOLETE
S/N 0102-014-6601

SECURITY CLASSIFICATION OF THIS PAGE (When Data Entered)

Block 20 Continued:

intercomparisons between the FGGE observed cyclone and the LFM model predictions are made. Destabilization that is found during cyclogenesis is a maximum during the early time periods. The LFM fields did not develop the intensity, strength, or depth of circulation that is found in the observed FGGE data. This may be linked to a poor representation of the diabatic processes in the LFM model.

Approved for public release, distribution unlimited

Application of Quasi-Lagrangian Diagnostics and FGGE Data in a Study of East-Coast Cyclogenesis

by

Donald A. Roman
Lieutenant Commander, United States Navy
B.S., State University of New York, Maritime College
at Fort Schuyler, 1970

Submitted in partial fulfillment of the
requirements for the degree of

MASTER OF SCIENCE IN METEOROLOGY
AND OCEANOGRAPHY

from the

NAVAL POSTGRADUATE SCHOOL
September, 1981

ABSTRACT

This synoptic study of an explosive deepening event, the Presidents' Day Storm of 17-20 February 1979, introduces and examines the Level III-b FGGE data in an oceanic storm. It applies the quantitative quasi-Lagrangian diagnostics techniques to both the FGGE data for a 48-hour period and a 24-hour LFM II prediction.

Using a mass budget analysis in isobaric coordinates, the mass structure and circulation intensity are examined and intercomparisons between the FGGE observed cyclone and the LFM model predictions are made. Destabilization that is found during cyclogenesis is a maximum during the early time periods. The LFM fields did not develop the intensity, strength, or depth of circulation that is found in the observed FGGE data. This may be linked to a poor representation of the diabatic processes in the LFM model.

TABLE OF CONTENTS

LIST OF TABLES

LIST OF FIGURES

ACKNOWLEDGEMENTS

The author wishes to express sincere appreciation and thanks to Dr. Carlyle H. Wash for his encouragement, guidance and patience as both an instructor and a thesis advisor. I am deeply indebted to him for his assistance and support during the preparation of this thesis.

Additionally, the author is indebted to the second reader, Dr. Russell Elsberry, for his careful renovation of the document. Dr. Scott Sandgathe deserves special thanks. Although he was deeply involved in his own research and manuscript preparation, he was always available for discussion and assistance. Michael McDermet has earned a special thank-you for his many efforts in obtaining reference products from the archives, as well as his instruction and material support in the preparation of the graphics. Lastly, the author wishes to thank all the faculty, professors, and staff who continually encourage and support the students in their efforts.

I. INTRODUCTION

East coast cyclogenesis has long been a subject of both scientific and practical interest. These rapidly developing storms exhibit great vigor. They can and often do produce significant weather that impacts on population centers, as well as producing adverse off-shore conditions hostile to the mariner. The object of this case study was an intense cyclone that developed off the east coast of the United States during the period of 18-21 February 1979. Due to occurrence during a holiday period, it was titled the Presidents' Day Storm. It produced both heavy precipitation and off-shore winds in excess of sixty knots.

As a result of this long standing interest, there exists a number of excellent studies of east coast cyclogenesis. Two of the more recent, Danard and Ellenton (1979) and Sanders and Gyakum (1980), are of particular note. Interestingly, these excellent works contain some conflicting views. Danard and Ellenton (1979) state, "Prognoses of east coast cyclogenesis for four time intervals all gave the same somewhat startling result: input of heat and water vapor from the sea surface did not contribute significantly, at least while the Low was deepening rapidly." In essence, their work tends to highlight frictional drag influences, and relegates surface heating and water vapor fluxes to a secondary stature.

They indicate that these factors may tend to help prepare the stage, but do not assist the deepening process itself. In contrast, Sanders and Gyakum (1980) conclude, in part, "... that an adequate representation of the planetary boundary layer and of the bulk effects of cumulus convection is a necessary physical ingredient, missing in the NMC models." They further link the explosive deepening events to strong sea surface temperature (SST) gradients. One can conclude that the role of sensible and latent heat, cumulus activity and water vapor concentration is not adequately known for these east coast cyclogenesis events. Indeed, the dynamics and workings of these storms remains unresolved.

The Presidents' Day Storm is an extraordinary example of east coast cyclogenesis. Specifically, of particular note are the following observations:

1. Classic east coast cyclogenesis location;
2. Extraordinary strength of the high pressure system that dominated the east coast during the initial periods;
3. Anomalously intense coastal front;
4. Rapidity and strength of intensification;
5. Record precipitation;
6. Exceptionally poor performance of the current numerical models in prediction;
7. Availability of First GARP (Global Atmospheric Research Program) Global Experiment (FGGE) data to assist in the analysis of the storm.

This is not an exhaustive list, but it does impart a feeling for the unique nature of this event. A quick view of the storm's physical appearance helps define the dramatic development (Figure 1).

Already the Presidents' Day Storm has generated several informative discussions of its development. Bosart (1981) and Uccellini, Kocin and Wash (1981) have investigated the nature of this event. However, these studies reflect distinct differences in philosophy, and hence in approach, emphasis and analysis. Both discussions are essentially synoptic in nature and are designed to emphasize particular aspects of the Presidents' Day Storm. Bosart (1981) deals with the Presidents' Day Storm as a sub-synoptic event with emphasis on the role of the coastal front. He clearly illustrates the importance of the coastal front and emphasizes the strong contributions of surface fluxes of heat and moisture and convective activity. Uccellini, et.al. (1981) develop a jet streak analysis and tend to emphasize the ageostrophic nature of the low level jet that developes, and its interaction with the upper level flow pattern prior to cyclogenesis.

Continuation of the Presidents' Day Storm studies is clearly warranted. There still exists a need to quantify the storm and its dynamics in a more objective format. Quasi-Lagrangian Diagnostics (QLD) as currently developed (Wash, 1978) provide a useful approach. This thesis will pursue a more structured and clearly defined approach to the

Presidents' Day Storm through the use of Quasi-Lagrangian Diagnostic budget analyses. QLD utilizes a spherical budget volume which translates with the storm, or whatever phenomenon is under consideration. This allows fluxes across the boundary to be examined with any distortion due to storm translation removed (Appendix C). Further, these studies can be performed on the prognostic products, as well as on the analysis. This should allow some objective statements on model simulation of the storm's dynamics and allow further insights into the model performance. Wash (1978) has demonstrated the validity of this approach to model diagnostics, and applied QLD use on poor model predictions. One of the primary goals of this work is to utilize the QLD tools in a structured approach to the Presidents' Day Storm dynamics. The Presidents' Day Storm provides an opportunity to employ the QLD tools on a current phenomena where normally skillful numerical weather products were found lacking.

The Presidents' Day Storm is a representative cyclogenesis event that has a large body of supporting data. It occurred during one of the special observational periods of the First GARP Global Experiment (FGGE) where considerable additional data were collected. The resulting FGGE data sets are therefore available to expand and refine the normal data. These data sets were made available through the cooperation and resources of Dr. Louis Uccellini, NASA/Goddard Space Flight Center. Previous studies of east coast cyclogenesis

and oceanic weather systems have suffered from the lack of adequate data. Once an analysis is extended past the immediate coastal areas, individual case studies become extremely difficult due to the subjectivity that inherently intrudes into the analysis. FGGE data shows the promise of ending this restriction. This data set is supplemented with satellite soundings, ocean buoy data, aircraft winds and observations, and ship data that are not available in other data sets. Level III-b FGGE data have been objectively analyzed and should both improve the analysis and accurately extend it over the open ocean areas. Another primary goal of this study is to explore the skill of the FGGE data set in an over the ocean case study. Although the FGGE data sets have been utilized in numerical modeling experiments, this is believed to be one of the first utilizations of these data in a mid-latitude storm case study. Consequently, the synoptic data file currently available to assist investigation into this storm is exceptional.

II. ENVIRONMENTAL DATA AND SYNOPTIC SUMMARY

A. DATA BASES AND ANALYSES

In studying the Presidents' Day Storm two data bases and four sets of analyses have been utilized. The two data bases are the:

1. Limited Fine Mesh (LFM) fields from the National Meteorological Center (NMC); and
2. First GARP Global Experiment (FGGE) data obtained from the National Atmospheric and Space Administration (NASA) as prepared by the European Center for Medium Range Forecasts.

A complete listing of the time periods utilized and the individual fields available for each time period, per data base, is found in Table I, which also contains an interpretation key for the notation used throughout this study. The four sets of analyses are:

1. LFM;
2. FGGE;
3. Fleet Numerical Oceanography Center (FNOC); and
4. Bosart (1981).

The primary use of the data bases will be in the application of QLD for studying the storm's budget fields for varying time periods. The primary use of the various analyses will be in examining the representativeness of the FGGE data prior to QLD storm analysis.

Those Fleet Numerical Oceanographic Center analyses utilized are:

1. FNOC Sea-Level Pressure Analysis...The Northern Hemispheric Strip;
2. FNOC upper-air analysis for the 250 mb level;
3. FNOC Sea-Surface Temperature Analysis;
4. FNOC Optimum Track Ship Routing Analysis.

A complete description of the FNOC products can be found in the U. S. Naval Weather Service Numerical Environmental Products Manual, NAVAIR 50-1G-522.

B. FGGE DATA

This study utilizes the Level III-b FGGE data which represents a major meteorological effort. FGGE data taken during the Global Experiment were analyzed on a six hour basis. The Presidents' Day Storm occurred during a special observational period and, as a result a very complete data set was analyzed. This FGGE data set has several advantages relative to conventionally available data:

1. FGGE data is a computer analyzed data base that is global in nature and of high resolution (1.875 degrees in both longitude and latitude);
2. A major effort was made to improve the global data base, particularly in data sparse regions;
3. The FGGE data set represents an objectively analyzed global product capable of incorporating various data sources and off-time reports not currently available;
4. As a data base, the FGGE data set has been and is being used in numerous numerical modeling experiments and tropical studies. Its use for the synoptic study of mid-latitude ocean cyclones is largely untapped.

The FGGE Level III-b data set was derived using a three-dimensional multivariate optimum interpolation analysis. The analysis on 15 standard pressure surfaces on a non-staggered grid, having produced a first guess field from a nonlinear high resolution model, then incorporates new data. Observations are incorporated using a four-step quality control. A format check is followed by a gross error check against the first guess field. The last two checks are against neighboring data and preliminary interpolation to the observation point. Appendix B contains a more detailed description of the analysis scheme.

The Level III-b FGGE analysis produces five fields at the 15 standard heights from 1000 mb to 10 mb. These fields are height, U and V wind components, temperature and vertical velocity. Relative humidity is carried only to the 300 mb level (Table I).

The data coverage for the period of the Presidents' Day Storm is shown in Figures 2, 3 and 4, which are obtained from the "Global Weather Experiment, Daily Global Analysis, Part 1" published in April 1981 by the European Center for Medium Range Weather Forecasts. These figures illustrate that the geographic area of the Presidents' Day Storm is well covered by synoptic reports, upper air reports, ship reports, and drifting buoy data. Satellite coverage, although available, leaves something to be desired in the Presidents' Day Storm area. It is of major significance

that these data are incorporated and analyzed objectively. Previous to FGGE, most of the off-time upper air, ship, buoy, and satellite wind data would have been incorporated by hand analysis. Bosart (1981) demonstrates the superior skill of such an analysis in his study of the Presidents' Day Storm. However, the FGGE data represents an objectively analyzed collection of global data that could eventually be utilized to produce real time products which laborious hand analyses can not do. Having looked at the data coverage and quickly at the analysis scheme, attention is now focused on the FGGE analysis.

Are the FGGE data fields representative? In this thesis only a subjective answer can be formulated. The actual observations for this period were not available in time for this study, so there can be no close scrutiny of the data. Only the FNOC sea level pressure analyses and the FNOC upper-air analyses present any actual observations. As a result, the representativeness of the FGGE data will be quickly explored by a comparison of analyses with the FNOC products, and an examination of the pressure fields for consistency and representation of the features. Knowing that the data base is enhanced relative to the plotted data on the FNOC analyses, one can examine the representativeness of the finished fields. First, the surface comparisons will be presented using the FNOC and FGGE fields and then the upper level flow fields at 250 mb will be compared.

Examining the sea-level pressure fields of 18 February 1979 (Figure 5) at 1200 GMT, the dominant feature is the high pressure over the United States. Both analysis have centered the high pressure system the same and present the same synoptic pressure pattern. Both fields show an inverted trough extending northward from Mississippi and indicate ridging down the east coast. The pressure gradient from the high center to Nova Scotia is the same for both fields. The pressure gradient from the high center to Cuba is the same, with similar patterns throughout the subtropical areas.

On 19 February 1979 at 0000 GMT (Figure 6), the high pressure system is represented similar to the analyses of 18 February. The low developing off Georgia is analyzed similarly. The trough over Ohio is represented by a closed isobar in the FGGE field and is not quite closed in the FNOC field, although the associated pressure gradient is similar. Pressure patterns over the Atlantic Ocean are the same except for the trough which extends approximately 2 degrees farther south in the FNOC product.

Figure 7 displays the sea-level pressure fields of 19 February 1979 at 1200 GMT. The developing cyclone is depicted similarly and the surrounding pressure patterns are the same with the FNOC central pressure values slightly higher. East of the developing cyclone the high is almost 4 degrees further south and 4 degrees further east in the FNOC fields. However, if one examines the wind vectors in the FNOC analysis,

it can be seen that the dotted observations to the north and west of the high favor a placement further to the northwest and similar to the FGGE position. These dotted reports have been rejected in the FNOC analysis and so the resultant position is more to the east and south. It is concluded that the FGGE data is more consistent on this point. The trough in the Atlantic is analyzed the same.

In the 20 February 1979 analyses at 0000 GMT (Figure 8), the cyclone is depicted more symmetrical in the FNOC field, probably due to a smoother contouring routine. The high pressure centers east and west of the cyclone are similar with the FGGE field showing the eastern high slightly farther to the south. The FNOC field shows stronger ridging to the south of the cyclone, extending almost 10 degrees further east at 28°N.

Presentation of the 250 mb level fields begins at 1200 GMT on 18 February 1979 (Figure 9). Here the analyses show the pattern over the central United States similarly, but with slightly stronger flow in the FNOC fields. The trough along 55°N is very similar and is smoother in the FGGE fields between 25°N and 30°N. The FGGE fields show more zonal flow and less northerly wind component over the Great Lakes and New York area.

On 19 February 1979 at 0000 GMT (Figure 10), the FNOC field shows a more cohesive flow of the subtropical jet further north in the Texas region, but the pattern is

generally the same. Both fields capture the trough over the Great Lakes area. The FGGE fields remain more zonal over the eastern seaboard and eastward to approximately 60°W. The trough at approximately 55°W is depicted similarly.

Figure 11 displays the 250 mb fields of 19 February 1979 at 1200 GMT. In these fields the flow over the entire United States and the eastern seaboard are very closely matched. The trough at approximately 45°W is well represented by both fields. This time period comparison shows very little difference between the analyses.

The 250 mb fields of 20 February 1979 at 0000 GMT are presented in Figure 12. The FGGE field shows troughing off the east coast at 40°N and 70°W, much more clearly than does the FNOC field. However, both fields agree very closely over the United States. The FGGE field is more zonal between 20°N and 30°N and 50°W to 60°W, with the FNOC fields showing a more northerly component.

Lastly, the 250 mb fields of 20 February 1979 at 1200 GMT are viewed (Figure 13). The troughing along 60°W is more smoothly depicted in the FGGE analysis. The remaining portions of the fields compare very well over both the United States and the oceanic areas.

Although subjective, the above comparisons indicate that the FGGE fields are a reasonable representation of the surface and upper level flow. They compare very favorably with the available Fleet Numerical Oceanography Center

analyses and preserve height and pressure fields at the levels examined. The FGGE fields do demonstrate consistency over the ocean in the depiction of various synoptic features. Having examined the representativeness of the FGGE analyses, in the next secion this data set is utilized in a brief synoptic overview and analysis of the Presidents' Day Storm.

C. SYNOPTIC OVERVIEW

Both Bosart (1981) and Uccellini, et.al. (1981) have developed excellent synoptic summaries of the Presidents' Day Storm. For more detail of the storm, the reader is directed to these two studies. However, an abbreviated synoptic overview based on the FGGE data analysis will serve to highlight several important features and developments, as well as form the basic background for these studies.

1. 18 February 1200 Greenwich Mean Time (GMT) (Figure 14)

    a. The east coast is dominated by extreme cold and unusually strong high pressure.

    b. Pressure ridging east of the Appalachians is beginning to extend to the south and is conforming more closely to the eastern slopes.

    c. The 850 mb high pressure becomes more sharply defined than previously and troughing moves into the Mississippi Valley.

    d. The 500 mb trough moves into the Mississippi Valley.

2. 19 February 0000 GMT (Figure 15)

    a. High pressure remains over the east coast.

    b. A surface low begins to develop off the coast of Georgia.

c. Pressure ridging along the eastern slopes becomes better defined.

d. The coastal front (Bosart, 1981) is forming.

e. Active weather begins to concentrate in the narrow coastal region and eastern slopes.

f. Eastern surface and southeasterly flow at 850 mb are clearly evident north of the surface disturbance.

3. 19 February 1200 GMT (Figure 16)

a. The surface chart reflects cyclogenesis with the low center off the Virginia coast.

b. Intense precipitation areas are located in the middle Atlantic states as Bosart (1981) points out, and tends to be centered parallel to the coastal areas of the Chesapeake Bay area and the coastal front.

c. The 500 mb trough has moved east and has a classic alignment with the surface disturbance.

4. 19 February 1800 GMT (Figure 17)

a. Extraordinary cyclogenesis develops with the central pressure analyzed at 992 mb by Bosart (1981) and at 1000.6 mb in the FGGE analysis.

b. Surface pressures have fallen an incredible 26 mb in just 18 hours. Even the more conservative FGGE data indicates a 19 mb change, and an additional 6 mb pressure fall occurs in just six hours.

c. The 500 mb trough remains approximately as deep, but has moved to within approximately 5 degrees of longitude west of the surface disturbance.

The role of the high pressure system that dominates the east coast is basic to the synoptic discussion. An extremely intense high dominates both the surface (1048 mb) and 850 charts throughout the period until the 19 February 0000 GMT analysis. The southerly elongation along the eastern slopes

and its extension off-shore clearly define the baroclinic zone that is associated with the coastal front. The strength of this high clearly limited the intensity and eastward movement of the upper level trough. What role this high had in "preparing" the marine boundary layer in advance of the surface low is open to investigation.

The development of the low off the coast of Georgia and its movement north are similar to one case study of Danard and Ellenton (1980). It is interesting that both storms experienced maximum deepening off Cape Hatteras. However, the Presidents' Day Storm traveled along the coast over water, while Danard's case of 1 February 1976 did not proceed off-shore until it was north of Cape Hatteras.

The interaction of the Presidents' Day Storm surface low and the Ohio Valley upper level low is complex and is well described by Uccellini, et.al. (1981). The southern low moving northward provides an extremely strong easterly flux of moisture directed toward the coastal front and in advance of the movement of the upper level low. The upper level low interaction with the surface system is apparently directly linked to the explosive deepening of the system on 19 February (Uccellini, et.al. 1981). This interaction helps delineate some of the active weather areas prior to and during the cyclogenesis of 19 February 1979.

The LFM II prognostic products perform poorly. The 24 and even the 12 hour forecasts valid at 1200 GMT on

19 February have not begun to capture the cyclogenesis or the coastal pressure gradient. Figures 18 and 19 display the various products' storm positions. The placement of the low center by the LFM is too far to the south. The significance of the sea surface temperatures will be discussed shortly.

D. SYNOPTIC ANALYSIS

There are two primary techniques of analysis to be taken in this study. The first will be a plan-view and synoptic study of available data fields, and second, a quasi-Lagrangian diagnostic budget analysis of available data fields.

Plan-view studies are fairly self-explanatory, subjective and can generally only be used to infer features of interest. The following section presents essentially a synoptic overview of various data fields for the insights contained. Specific areas to be considered include; the comparison of the Presidents' Day Story as shown in FGGE data with the east coast cyclogenesis development as described by Sanders and Gyakum (1980), and an examination of the temperature fields at various heights in relation to the surface low.

It is of interest that the Presidents' Day Storm has every major characteristic discussed by Sanders and Gyakum (1980). The Presidents' Day Storm is a western ocean maritime event that occurred during the winter months. Indeed, the character of the storm is clearly hurricane – like at

1800 GMT on 19 February 1979, as Bosart (1981) shows with "warm core characteristics". The time of explosive deepening of the Presidents' Day Storm would cause it to be one of the storms that Sanders and Gyakum (1980) would miss. They considered only pressure changes between 1200 GMT analyses, which they point out might miss some deepening storms. The Presidents' Day Storm experienced a 1200 to 1200 GMT drop in pressure of 0.62 mb per hour from 18 to 19 February 1979, where as the decrease was 1.1 mb per hour from 0000 to 0000 GMT between 19 to 20 February 1979. Considering the latitude correction, (sin(lat.)/sin(60)x1 mb), which yields a 0.66 mb/hour fall required, the 1200 to 1200 GMT drop does not meet the criterion, whereas the 0000 to 0000 GMT drop does. If the 12 hour drop in central pressure is considered the Presidents' Day Storm exceeds the Sanders and Gyakum (1980) criterion.

The Presidents' Day Storm also displays the more subtle characteristics required for development. It develops within 300 to 400 nm of a 500 mb trough as observed in Figures 16 and 17. This upper-level trough travels a significant distance while the surface low displays little lateral movement prior to and during development. This surface low movement can be examined in Figure 19, which also displays sea-surface temperatures. It is evident that the Presidents' Day Storm satisfies the location requirement of being in or near the intense sea-surface temperature gradients, within

or north of the, "warm waters of the Gulf Stream." In short, the Presidents' Day Storm clearly belongs to that class of storms that Sanders and Gyakum (1980) believe requires further representation of the, "...bulk effects of cumulus convection..." within the NMC forecast models.

The vertical temperature structure shown on Figures 20 and 21 indicates an interesting contrast. Notice that the fields at 1200 GMT 19 February 1979 exhibit the expected pattern. The warm air is located to the east and south of the low and there is cold air to the west and northwest. There does not appear to be large vertical development. The same fields at 1800 GMT, just six hours later, show an almost circular warm region that is remarkably symmetrical and is vertically aligned with the surface low. This is a somewhat startling structure, especially considering the rapidity with which it appeared. It is suggestive of deep intense cumulus activity over a large area, because the same feature is distinguishable to the 500 mb level. This vertical alignment is also found in the fields for 20 February at 0000 GMT; however, it is not as well defined as in Figure 21 and has lost some symmetry. The convective activity is visible in the satellite coverage for this time period (Bosart, 1981). Clearly, diabatic effects are to be looked for in the QLD analysis.

III. QUASI-LAGRANGIAN DIAGNOSTICS ANALYSIS

A. QUASI-LAGRANGIAN DIAGNOSTICS

One of the primary goals of this thesis is a more objective approach to synoptic storm studies. The analysis techniques of QLD will be used to achieve this goal. This next section will be used to describe the basic mechanisms of QLD, and to describe the QLD mass budget output available for analysis.

Quasi-Lagrangian Diagnostics are a volumetric approach to cyclone study. In this approach, a cylindrical volume is established on the earth's surface and is centered on the low pressure center. Unlike many budget studies, the volume is not stationary. It follows the storm traveling at the same course and speed. Having established the volume, it is then possible to study the budget of a desired quantity. It is necessary to consider the transport into and out of the volume, plus any internal sources of sinks. Storm properties, such as angular momentum, mass, kinetic energy, potential energy, vorticity or moisture may be studied. Time constraints will restrict this thesis to applying QLD techniques to a mass budget study in pressure coordinates of the Presidents' Day Storm. While the mass budget is the simpliest budget to formulate, there are several studies in which more advanced budgets are examined. Examples of some recent

studies are found in Table II, after Wash (1978). A description of the general QLD transport equations that are applicable to any desired quantity is found in Appendix C. Wash (1978) develops the budget equation, as well as the programmed format for the budget study developed in this thesis.

The volume's lateral boundaries will be specified in terms of degrees latitude at the specified storm position. In this way, radials will mark a convenient distance scale, as well as a boundary. The bottom boundary is normally defined as the earth's surface, and the upper boundary is considered to be the 100 mb level. The later assumption is generally very good as the 100 mb level is normally well above most tropospheric disturbances in the mid-latitudes and there will not be significant vertical transports at that level.

The mass budget study has simple boundary conditions. The vertical velocity equals zero at the lower and upper boundaries, that is, there is no vertical mass flux across these boundaries. These conditions allow the general equations of Appendix C to be simplified. Referring to the definitions and notation of Appendix C, the equations are now expressed as:

$$dm/dt = L.T. = \int_{\eta_B}^{\eta_T} \int_{0}^{2\pi} 1/g(U-W)_{\beta} r \sin \beta_B \, d\alpha d\eta \Big|_{\beta_B}$$

$$V.T. = \int_{0}^{\beta_B} \int_{0}^{2\pi} 1/g\left(\frac{d\eta}{dt} - \frac{d\eta_B}{dt}\right) r^2 \sin\beta \, d\alpha \, d\beta \Big|_{\eta}$$

Here dm/dt refers to the total change of mass with respect to time. It is the mass tendency. L.T. is the lateral mass transport, and V.T. is the vertical mass transport.

The first equation above represents the net lateral convergence/divergence of mass flux into or out of the volume. Once the lateral transport field is known, the vertical mass transport required to support this lateral flux can be established. The most accurate data field available is the sea level pressure. We can use the required pressure field to "force" our integrated lateral transport result to agree with the known mass changes in the storm's budget volume. This is necessary because our initial integration will not yield the mass transport necessary to produce the known pressure field. It will have a residual due to the imperfect data fields. Using a mass weighted scheme that corrects upper levels more than the lower levels (O'Brien, 1970) the residual is compensated throughout the volume and a corrected lateral mass transport is used via the vertical transport equation to develop the vertical flux fields. This is possible because there is a zero transport across the volume's vertical boundaries. This vertical flux is then expressed as

a vertical velocity field with upward motion defined as positive.

The QLD mass budget calculations do provide some direct fields of data to be examined, as well as various derived fields. The primary fields are:

1. Both the U and W mass transport terms, where U is the relative flow component normal to the volume and W is the translational velocity component that is normal to the volume.

2. The uncorrected lateral mass transport, which is the net U - W lateral mass transport before the correction of the integration.

3. The mass tendency, which is the total change of mass with respect to time.

4. The mass residual, which is the residual from the integration process due to the comparison of the uncorrected lateral mass transport and the required mass tendency.

5. The mass transport correction, which is the correction applied to the lateral mass transport using the O'Brien (1970) technique.

6. Total corrected lateral mass transport, which is a primary field of interest as it represents the computed lateral mass transport after it has been corrected. It is this term that represents net convergence/ divergence.

The derived fields of interest are the area-averaged potential temperature fields, and the area-averaged vertical velocity fields.

The uncorrected mass transport can give a preliminary indication of preferred levels of inflow and outflow. The corrected mass transport will determine the preferred inflow and outflow regions, and the lateral branches of the cyclonic

mass circulation. The vertical velocity fields will provide an indication of the structure and strength of the storm's vertical transport. Lastly, the area-averaged potential temperature fields will be examined for stability structure.

The lateral mass transport will be expressed as an averaged transport into or out of a layer, for example, the 1000 to 850 mb layer. The vertical velocity is an average value for a given level. The potential temperature field is taken from the actual temperature data for a given level and is an area-averaged value.

B. QUASI-LAGRANGIAN DIAGNOSTICS ANALYSIS

Quasi-Lagrangian Diagnostics were completed on both the FGGE and the LFM II fields. The FGGE analysis starts at 1200 GMT on 18 February and runs for 48 hours in six hour increments. The LFM II analysis starts at the same time but runs for only 24 hours in six hour increments. It is unfortunate that the storm is no longer located on the LFM grid beyond 1200 GMT on 19 February, and that budget data could not be prepared beyond this time. However, meaningful comparisons can be made within the time periods available.

The storm tracks based on the FGGE and the LFM analyses are presented in Figure 22. An important part of the QLD technique is to consider the storm volume based on that product's storm track. In this way, the storm property is studied pertinent to that particular product's storm volume.

The difference in storm tracks between the FGGE observed and the LFM II cyclones is small in this case and does not prevent a comparison of the budget analyses for the FGGE and LFM data (Figure 22). Both tracks begin at the same location at 1200 GMT on 18 February 1979. This point is where the closed low first becomes distinguishable at 0000 GMT on 19 February. This is considered a reasonable compromise for two important reasons:

1. It provides a well defined starting position for the analysis scheme; and
2. It ensures that the initial area of development is scrutinized by the analysis scheme at the very onset of development.

The area that is considered by the QLD analysis expands with radial distance from the pressure center. Radius 5 equates to 300 nm, whereas radius 10 is a 600 nm radius circle. The corresponding areas are illustrated in Figure 22.

The QLD analyzed fields examined consist of the area-averaged potential temperatures, the corrected lateral mass transport fields, and the area-averaged vertical velocity fields. Both the vertical velocity fields and the mass flux fields are calculated over six hour increments in the QLD analysis scheme.

The QLD area-averaged potential temperature and stability fields presented in Figures 23-26 will be examined for possible indications of diabatic effects. Figure 23 and 24 display vertical difference in potential temperature for the LFM and

the FGGE data at radii 5 and 7. This difference is the simple difference of the top level potential temperature minus the bottom level potential temperature. This gives an indication of the temporal variation in static stability within a given radius. This analysis yields the following results:

1. There is a destablization tendency apparent throughout the storm;

2. The FGGE data displays less destabilization between 1000/850 mb, but more between the 850 and 700 mb levels, when compared to the LFM;

3. The destabilization effect is most pronounced within the first six hours of the storm. This is the period that leads to the development of a distinguishable surface low, and is approximately twelve hours in advance of the storm's period of maximum development;

4. The FGGE data retains more stability than the LFM in the lower layers.

Area-averaged potential temperature fields were examined in an attempt to isolate the cause of the initial destabilization. Isentropes for radius six, which is representative of other radii, are displayed in Figure 25. The mean potential temperature fields show that the initial stabilization effect is due to surface warming. This low level increase in potential temperature is present in both the FGGE analysis and the LFM prediction from 1200 to 1800 GMT on 18 February 1979. The high surface temperatures are present for the next 12 hours and are followed by a cooling period. The LFM shows a higher surface temperature than does the FGGE analysis.

In the mid and upper troposphere, the mean potential temperature shows little temperature change during the first 12 hours and a subsequent cooling throughout the troposphere. This decrease in potential temperature was surprising in view of the convective character of the cyclone, and in light of the warm tongue that developed in the low troposphere (Figure 21). It is believed that advective cooling, at radius six, particularly associated with the 500 mb trough west of the cyclone, overwhelms any warming due to the convective processes near the storm center. Time constraints prohibited detailed examination of the temperature structure at the smaller radii.

To complete the analysis of the cyclone's stability, the low troposphere is considered in a single layer from 1000 to 500 mb. These fields are examined to provide an analysis of the temporal changes in static stability in a format that is comparable with a numerical simulation of oceanic cyclogenesis by Sandgathe (1981). Figure 26 presents the 500 - 1000 mb stability results for radii 5 and 7, with the FGGE and LFM data exhibited together at radius 6 in Figure 27. A destabilization trend is present throughout the storm for both the 24 hour LFM predicted field and the 48 hour FGGE analysis. The first 6 hour time period again produces the most pronounced reduction in static stability. The stability decreases approximately 1 degree/100 mb in the LFM data and 1.5 to 2.0 degrees/100 mb for the FGGE data. This is

considerably more than the stability changes presented by Sandgathe (1981), who found decreases of less than 1 degree/ 100 mb for a twelve hour period.

To summarize the stability analysis, the following major points were noted:

1. The FGGE data retains more static stability than the LFM data;

2. The initial destabilization is slightly more pronounced in the FGGE data;

3. The destabilization trend is continuous throughout the storm period;

4. The FGGE and LFM fields in the lower troposphere shows warming through 1200 GMT on 19 February and then cooling;

5. Destabilization is most pronounced in the first two time periods. That is not to say the columns are unstable, but rather that they become less stable. This decrease of static stability is consistent with recent numerical modeling studies which have also displayed a decrease in static stability approximately twelve hours prior to the period of rapid deepening (Sandgathe, 1981). In the analysis, this is not considered to be a result of land effects being included in the area-averaged potential temperature fields, as it does not increase with increasing land area at larger radii;

6. The potential temperature fields appear to disagree with the storm's temperature fields (Figure 21). This is believed to be a result of the radius over which the budget volume is area-averaged. Examination of Figure 21 reveals a warm core of approximately 4 degrees diameter, whereas the smallest radius considered in the budget study was 5 degrees. It is believed that smaller radii, perhaps one or two degrees, would more accurately describe the effects observed in Figure 21.

The QLD lateral mass transport analyses are included on Figures 28, 29 and 30. The lateral transport is examined first. Time sections of lateral mass transport for

representative radii are presented in Figures 28 and 29. Radii six and nine were chosen for the inner and outer radii respectively. The fields have been normalized so that they are in terms of grams per second per 100 mb and are multiplied by 10**-10 for plotting convenience. Positive values denote flux into the storm volume and negative is an outward flux. Both the FGGE data and the LFM model display a two layer circulation with the inflow region in the lower troposphere, a level of non-divergence in the mid-troposphere and the outflow region in the upper troposphere. Although the general structure is similar between the FGGE and the LFM analyses, there are differences in the details of the structure and in the intensity of the mass flow. The LFM model inflow region is confined to the lowest 200-250 mb region with the level of non-divergence remaining near 750 mb for the entire period. In contrast, the FGGE data set shows a lateral transport inflow regime that grows vertically during cyclogenesis, so that the level of non-divergence moves upward to approximately 600 mb by 1200 GMT on 20 February. The intensity of the inflow and outflow regimes increases in time with the FGGE data becoming nearly twice as large as the LFM. A similar lateral mass circulation is found at a larger radius of nine degrees (Figure 29). The LFM cyclone exhibits a shallower and weaker circulation than that exhibited by the FGGE data.

A detailed intercomparison of the transport structure is presented in Figure 30. Vertical profiles of the lateral transport for the representative radii are displayed for 1200 GMT on 19 February. The features discussed above are more apparent. The mass budget analysis shows strong differences in the cyclone circulations; weak and shallow circulation in the LFM model and more vigorous and deeper circulation in the observed FGGE vortex. The flux values are indicative of the vitality of the storm as the stronger the mass circulation, the stronger the inward transportation of moisture, vorticity and other storm properties. The FGGE lateral mass transport fields and the two layer circulation are consistent with the findings of Downey and Johnson (1978). The surface layer remains convergent throughout the storm, however the strength of the divergent flow aloft shows more variation. Interestingly, the Presidents' Day Storm begins to moderate on 20 February and then reintensifies on 21 February, as is also verified by the FNOC surface analysis. The FGGE data represents this moderation and clearly indicates reintensification at the later time periods on the 20th. Notice in Figure 29 that the divergent mass flux represented in the FGGE data moderates after 1800 GMT on 19 February at 275 mb. It reintensifies on 20 February. There is a corresponding variation in the lower level inflow, with the divergence aloft reintensifying slightly earlier than the lower inflow. This is consistent with strengthening divergence aloft,

surface deepening and developing a more intense surface circulation.

The QLD vertical velocity fields in Figures 31-33 represent the vertical mass transport field. The time section analysis will display an inner and outer radii with radii six and nine respectively. An examination of the area-averaged vertical velocity within radius six (Figure 31) shows the LFM maximum vertical velocity remains low in the troposphere at approximately 700 mb. In contrast, the FGGE data's level of maximum vertical velocity continually rises through the lower troposphere until it is at approximately 400 mb at 1200 GMT on 19 February. The flow of the FGGE vertical velocity is more intense; not necessarily in peak values, but in the depth of the circulation. During the first 24 hours the LFM vertical velocity at 300 mb is approximately 0.4 mb/sec, whereas the FGGE data is already about 1 mb/sec. Results at radius nine (Figure 32) show a similar difference in the level of maximum vertical velocity, but the magnitudes of the flow are more similar. Figure 33 presents the vertical velocity profiles of radii six and nine in a more convenient form. The deeper vertical field of the FGGE data is clearly seen, as well as the lower level of the LFM maximum.

In summary, the Quasi-Lagrangian budget studies with the FGGE analyzed data and the LFM model data have been used to

investigate the structure and mass circulation fields of the Presidents' Day Storm. The mass budget analysis and the vertical velocity analysis have revealed:

1. Shallow and weaker circulation in the LFM;

2. Deep, vigorous, and more intense circulation in the FGGE data;

3. Differences in the mass circulation consistent with a weaker cyclone being depicted in the LFM, and differences in the vertical velocity field between the LFM and the FGGE data are likely due to the diabatic parameterization of the LFM. These differences are interesting in light of recent research by Sandgathe (1981). His numerical modeling experiments indicate diabatic effects significantly increase vertical velocity fields compared to simulations without such effects. The vertical velocity comparison tends to indicate these strong diabatic effects may be present in the FGGE data, or perhaps better represented in the FGGE compared to the LFM data.

IV. RESULTS AND RECOMMENDATIONS

This thesis has accomplished the following:

1. Utilization of FGGE data in a synoptic cyclone study, and specifically in an explosively deepening oceanic event.

2. Introduction of the objective Quasi-Lagrangian Diagnostics techniques in synoptic studies at the Naval Postgraduate School.

3. Analysis of the mass budgets for the FGGE data and the LFM model data sets for the Presidents' Day Storm.

The mass budget studies for the Presidents' Day Storm, plus the limited comparisons between LFM and FGGE fields, yields some specific insights. There are several recurring results:

1. The LFM predicts development of the storm only during the first time periods;

2. The LFM does not develop a deep vertical structure that should accompany such an intense cyclone. The FGGE data clearly shows a rapidly growing inflow layer, a rising level of non-divergence and a vertical velocity field that rapidly develops upwards from the low troposphere. This structure is not present in the LFM forecast cyclone. The LFM storm circulation remains shallow with a low level of non-divergence;

3. The LFM mass flux is in some cases almost half of that developed in the FGGE data. It does not develop the vigorous mass circulation displayed by the Presidents' Day Storm;

4. There is some, but suprisingly little, evidence of low level heating or diabatic effects apparent. These data contain both adiabatic and diabatic effects and these can not be separated in a mass budget study of this type.

There are some recommendations that are a natural outgrowth of this thesis effort. First, this thesis only explored the mass budget of the Presidents' Day Storm, Additional quantitative studies of this storm are required:

1. A study in isentropic coordinates would be far more sensitive to possible diabatic effects in the storm. These studies need to include a close examination at both inner and outer radii;

2. Angular momentum and circulation studies are necessary to complete an objective analysis of the Presidents' Day Storm;

3. The QLD techniques should be applied to additional examples of east coast cyclogenesis so that a more complete and quantitative description of this important class of storms can be developed. This description should then be examined in light of the new Navy Operational Global Atmospheric Prediction System (NOGAPS) that becomes operational this year;

4. The structure of the Presidents' Day Storm clearly demonstrates intense vertical growth. This suggests cumulus and large scale convective mechanisms play a major role. Additional studies are indicated to determine the mechanisms necessary to enable numerical prediction of this class of storm. The LFM data set was less statically stable than the FGGE data set, although it included the observed destabilization trend. However, it did not adequately develop the observed vertical velocity or predict the observed deepening rates. These differences require specific description;

5. The budget analysis results need to be examined on a sector-by-sector basis to lessen the impact of area-averaging on the data. The sector results may more accurately resolve the contribution of the cumulus activity and land/sea heating differences within the storm volume;

6. The QLD techniques should be examined for possible use in the study of various ocean phenomena. These techniques are applicable to a large set of phenomena, and are not restricted to the atmosphere. Specific examples are strong western boundary current meanderings, ocean eddies and upwelling events. These phenomena could be readily studied if the data problems could be overcome.

APPENDIX A

COMMON ABBREVIATIONS AND ACRONYMS

ECMWF	European Center for Medium Range Weather Forecasts
FGGE	First GARP Global Experiment
FNOC	Fleet Numerical Oceanography Center
FNOCUA	Fleet Numerical Oceanography Center Upper-Air Analysis
GARP	Global Atmospheric Research Program
GMT	Greenwich Mean Time
LFM	Limited Fine Mesh
mb	millibars
NASA	National Atmospheric and Space Administration
nm	nautical mile
NMC	National Meteorological Center
OTSR	Optimum Track Ship Routing
QLD	Quasi-Lagrangian Diagnostics
SST	Sea Surface Temperatures
XPORT	Transport

APPENDIX B

LEVEL III-B FGGE DATA

The following information has been extracted from the Global Weather Experiment, the Daily Global Analysis, published by the European Centre for Medium Range Weather Forecasts, in April 1981. This section provides a more complete description of the FGGE data set than that contained in the thesis text. Level III-b FGGE data is:

> "...an intermittent data assimilation system consisting of a multivariate optimum interpolation analysis, a non-linear normal mode intialization and a high resolution model which produces a first guess forecast for the subsequent analysis. Data are assimilated with a frequency of 6 hours. The analysis consists of two parts, one for simultaneous analysis of surface pressure, geopotential height and horizontal wind, and another part for analysis of humidity.
>
> The mass and wind analysis is a multivariate, three-dimensional statistical interpolation using the observed deviations from a first guess forecast as the analysis parameter. The observations are assimilated in a consistent way through the assumption of geostrophically balanced forecast error covariances between geopotential height and the wind components. This causes the analyzed corrections to the first guess forecast, to be locally non-divergent and approximately geostrophic at high latitudes. Observed divergences of a scale larger than about 1000 km are however retained and analyzed in a realistic way. Hydrostatic balance is achieved through conversion of temperature observations into thicknesses prior to the assimilation.
>
> During the analysis, the observations are subject to a four step quality control containing format checks, and checks against the 6 hour first guess forecast, neighbouring data and finally a preliminary interpolation to the point of the observation. Those observations that deviate more than a certain threshold value, depending on the observation error and the first guess error, are rejected. A special record is kept of all rejected data, and a

condensed version of this information will be made available to users of the ECMWF level III-b data set.

The data set contains both basic analysis parameters as well as derived parameters. The basic analyses are uninitialized and consist of geopotential height, sea level pressure and horizontal wind components. The derived parameters are temperature, relative humidity and vertical velocity. The relative humidity is determined from the mean water content in each analysis layer (the basic analysis parameter for humidity) and the temperature. The vertical velocity, expressed in mb/sec, is calculated from initialized divergences..."

Additional details can be found in the above referenced text.

APPENDIX C

QLD STORM COORDINATES AND GENERAL TRANSPORT EQUATIONS

The following information is extracted from Wash (1978) to supplement the discussion of the Quasi-Lagrangian Diagnostics contained in the text. Essentially, this appendix will establish the coordinate system and the generalized transport equations.

The storm vlume used for the diagnostic scheme is established in spherical coordinates and has the following notation (Figure 34):

α---azimuthal coordinate

β---angular radial coordinate

r---position vector originating from the earth's center

R---position vector from the storm center to any point in the volume

k,l,m---unit vectors in the vertical, azimuthal and radial directions

U---wind velocity relative to the earth, U = dr/dt

W_0---horizontal velocity of the reference axix, $w_0 = dr_0/dt$

W---generalized boundary velocity at any point on the boundary

$$W = |W_0| \cos(\alpha - \alpha_0)$$

Using these coordinates, the volume is established, as well as the quasi-horizontal surfaces (Figure 34). These surfaces are called quasi-horizontal because of the slopes

present in isentropic coordinates. The storm budget volume is expressed by the following equations:

$$V_\eta = \int_{V_\eta} J_\eta \; r^2 \sin \beta dV_\eta$$

here

$$J_\eta = \left| \frac{\partial z}{\partial \eta} \right| \text{ and } dV_\eta = d\alpha d\beta d\eta$$

The budget of any property (F) takes the following form:

$$dF/dt = \text{Lateral Transport} + \text{Vertical Transport} + \text{Sources} + \text{Sinks}$$

The generalized lateral transport is:

$$L.T. = \int_{\eta_B}^{\eta_T} \int_0^{2\pi} \rho J_n \, (U-W)_\beta \, fr \sin \beta_B d\alpha d\eta \Big|_{\beta_B}$$

The generalized vertical transport is:

$$V.T. = \int_0^{\beta_B} \int_0^{2\pi} \rho J_n \left(\frac{d\eta}{dt} - \frac{d\eta_B}{dt}\right) fr^2 \sin\beta d\alpha d\beta \Big|_\eta$$

Sources or sinks are:

$$S = \int_{V_\eta} \rho J_n \frac{df}{dt} r^2 \sin \beta dV\eta$$

The above equations are the generalized equations and thus are not subject to boundary conditions. Further modification can be made depending on the coordinate system for the budget calculations. For hydrostatic conditions, the isobaric coordinates allow:

$$\rho J_p = \frac{1}{g}$$

here p is a pressure surface.

In isentropic coordinates: $\rho J_\theta = \frac{1}{g}\frac{\partial P}{\partial \theta}$

Observe that where F is defined as mass in pressure coordinates, the final form as utilized in this thesis is identified. Considering a unit mass, F = 1, the mass budget equation is:

$$\text{L.T.} = \int_{\eta_B}^{\eta_T} \int_0^{2\pi} \frac{1}{g} (U-W)_\beta \, r \sin \beta_B \, d\alpha d\eta \Big|_{\beta_B}$$

$$\text{V.T.} = \int_0^{\beta_B} \int_0^{2\pi} \frac{1}{g} \left(\frac{d\eta}{dt} - \frac{d\eta_B}{dt}\right) r^2 \sin \beta d\alpha d\beta \Big|_{\eta}$$

LIST OF REFERENCES

1. Chen, T. G., and Bosart, L. F., Quasi-Lagrangian kinetic energy budgets of composite cyclone-anticyclone couplets. Journal of Atmospheric Science, 34, 452-464, 1977.

2. Bosart, L. F., The Presidents' Day Snowstorm of 18-19 February 1979: A sub-synoptic scale event, Monthly Weather Review, 109, 1542-1545, 1981.

3. Danard, M. B. and Ellenton, G. E., physical influences on east-coast cyclogenesis, Atmosphere-Ocean, 18, 65-82, 1980.

4. Downey, W. K. and Johnson, D. R., The mass, absolute angular momentum and kinetic energy budgets of model generated extratropical cyclones and anti-cyclones, Monthly Weather Review, 106, 469-481, 1978.

5. Johnson, D. R. and Downey, W. K., The absolute angular momentum budget of an extratropical cyclone: Quasi-Lagrangian diagnostics 3, Monthly Weather Review, 104, 3-14, 1976.

6. NAVAIR 50-1G-522, U. S. Naval Weather Service Numerical Environmental Products Manual, published by direction of Commander Naval Weather Service Command, 1 June 1975, change 3 of 1979.

7. O'Brien, J. J., Alternative solutions to the classical vertical velocity problem, Journal of Applied Meteorology, 9, 197-203, 1970.

8. Sanders, F. and Gyakum, J. R., Synoptic-dynamic climatology of the "Bomb", Monthly Weather Review, 108, 1589-1606, 1980.

9. Sandgathe, S. A., A numerical study of the role of air-sea fluxes in extratropical cyclogenesis, Ph.D. Thesis, Department of Meteorology, Naval Postgraduate School, 1981.

10. Spaete, P., A diagnostic study of the available potential and kinetic energies of a mid latitude cyclone. M.S. Thesis, University of Wisconsin, 1974.

11. The Global Weather Experiment, Daily Global Analysis, Part I, published by the European Centre for Medium Range Weather Forecasts, April 1980.

12. Uccellini, L. W., Kocin, P. J., and Wash, C. H., The Presidents' Day Cyclone, 17-19 February 1979: An analysis of jet streak interactions, being reviewed for publication, Monthly Weather Review.

13. Wash, C. H., A momentum circulation budget for an extratropical cyclone, M.S. Thesis, University of Wisconsin, 1975.

14. Wash, C. H., Diagnostics of observed and numerically simulated extratropical cyclones, Ph.D. Thesis, Department of Meteorology, University of Wisconsin, May 1978.

TABLE I

FGGE AND LFM DATA

Time Periods Available

FGEE		LFM	
1800Z	1912Z	1812P0	1812P24
1812Z	1918Z	1812PA	1900P0
1818Z	2000Z	1812P6	1900PA
1900Z	2006Z	1812P12	1900P6
1906Z	2012Z	1812P24	1900P12

Data For Each Time Period

mb x 10...100	85	70	50	40	30	25	20	15	10
HEIGHTS	X	X	X	X	X	X	X	X	X	X
POT. TEMP.	X	X	X	X	X	X	X	X	X	X
VER. VEL.	X	X	X	X	X	X	X	X	X	X
REL. HUMID.	X	X	X	X	X	X				
U VEL. COMP.	X	X	X	X	X	X	X	X	X	X
V VEL. COMP.	X	X	X	X	X	X	X	X	X	X

1. Vertical velocity in pressure coordinates is only available in FGGE data.
2. LFM relative humidity is available for the surface only.

Legend Guide For Figures

PREFIXES: L = LFM FEB = FGGE
DATE-TIME GROUP: 1900 = 19 FEB '79 at 0000Z at 0000GMT
SUFFIXES: P0 = Observed
PA = Analyzed Data
P6 = Six Hour Prognostic
P12 = Twelve Hour Prognostic
Z = GMT

Example: L1812P6 yields the LFM product of 18 FEB '79 at 1200 GMT which is a six hour prognostic chart.
FEB 1912Z yields the FGGE field of 19 FEB '79 at 1200 GMT.

TABLE II

QLD BUDGET STUDIES [adopted from Wash, (1978)]

Property	Researcher(s)
Mass	Johnson and Downey 1976
Absolute Angular Momentum	Johnson and Downey 1976 Wash 1978
Available Potential Energy	Spaete 1974
Circulation	Wash 1975
Kinetic Energy	Chen and Bosart 1977

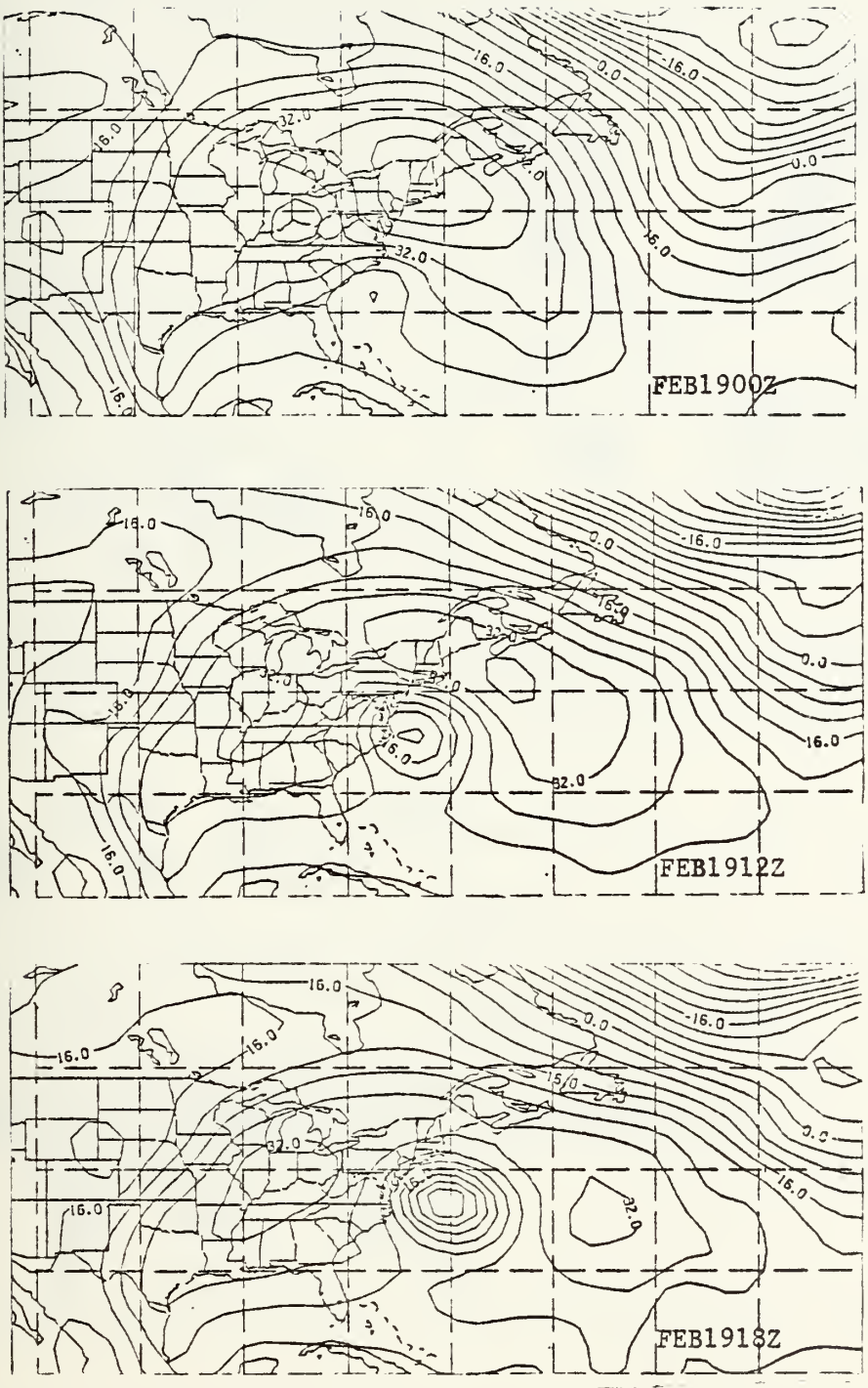

FIGURE 1. Surface pressure maps on 19 February 1979 at 0000, 1200 and 1800GMT. Contours are pressures-1000 mb.

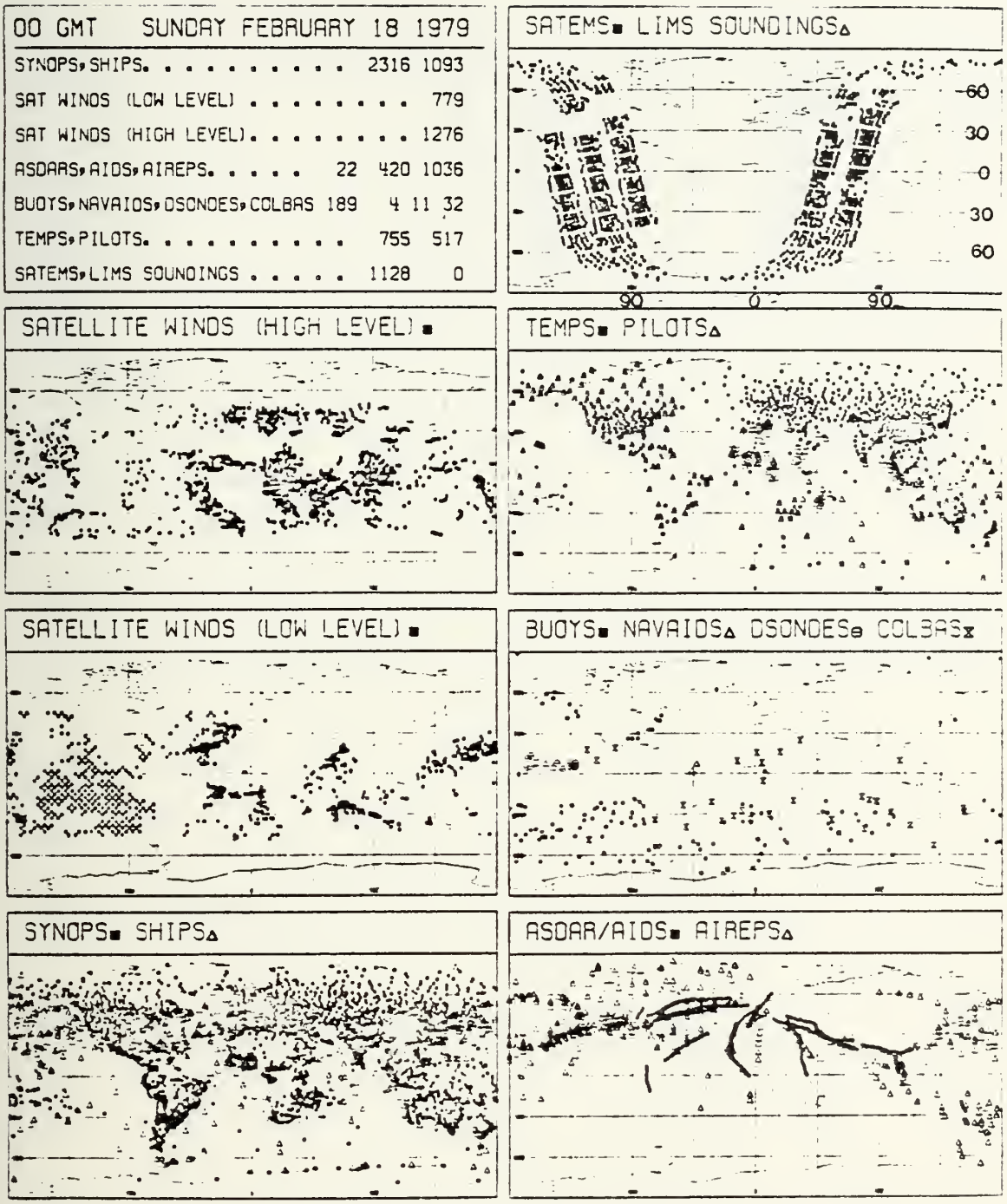

FIGURE 2. Representative data coverage of the Global Weather Experiment, for 0000GMT 18 February 1979, as published by the European Centre for Medium Range Weather Forecasts.

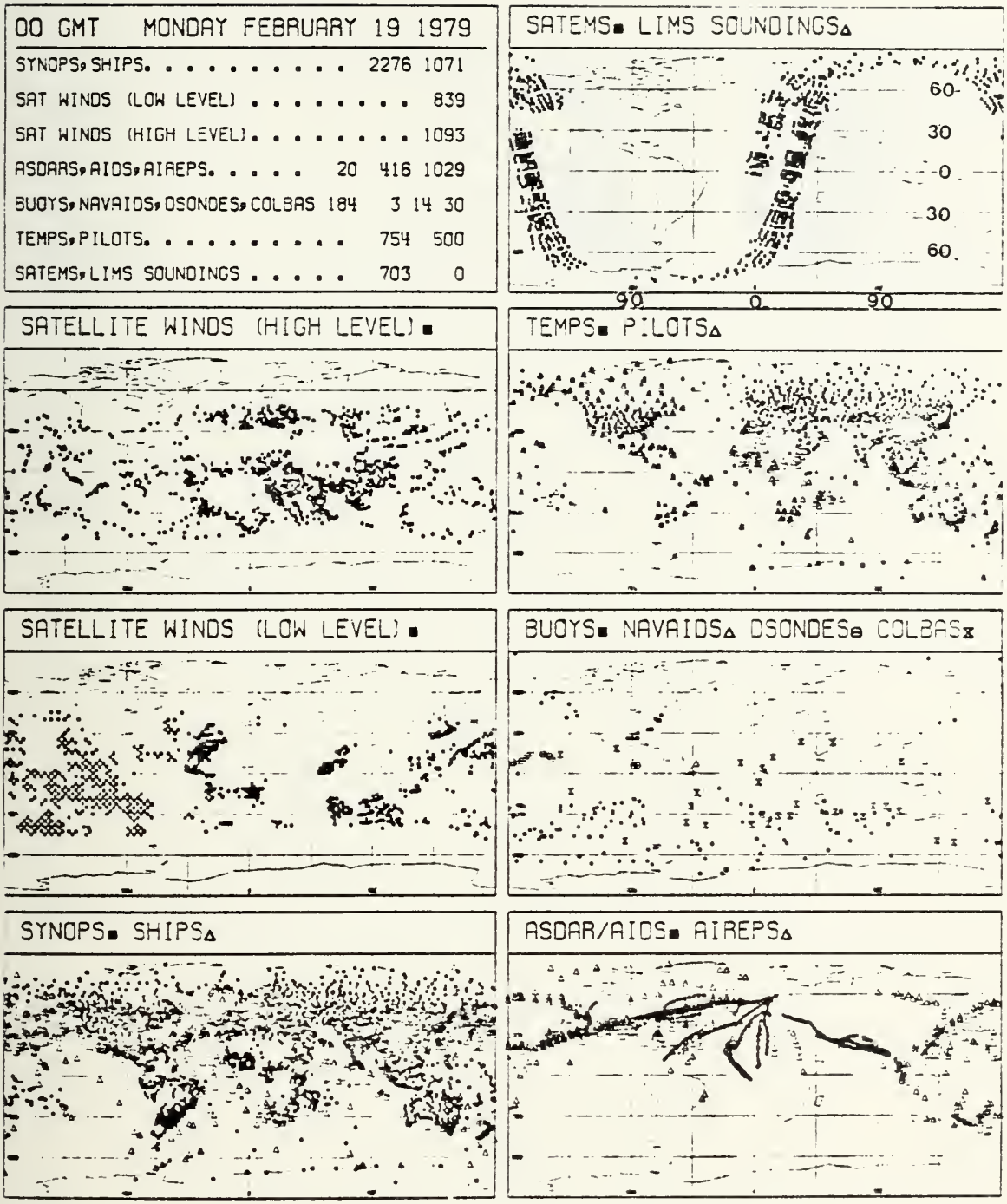

FIGURE 3. As in Figure 2 except for 0000GMT 19 February 1979.

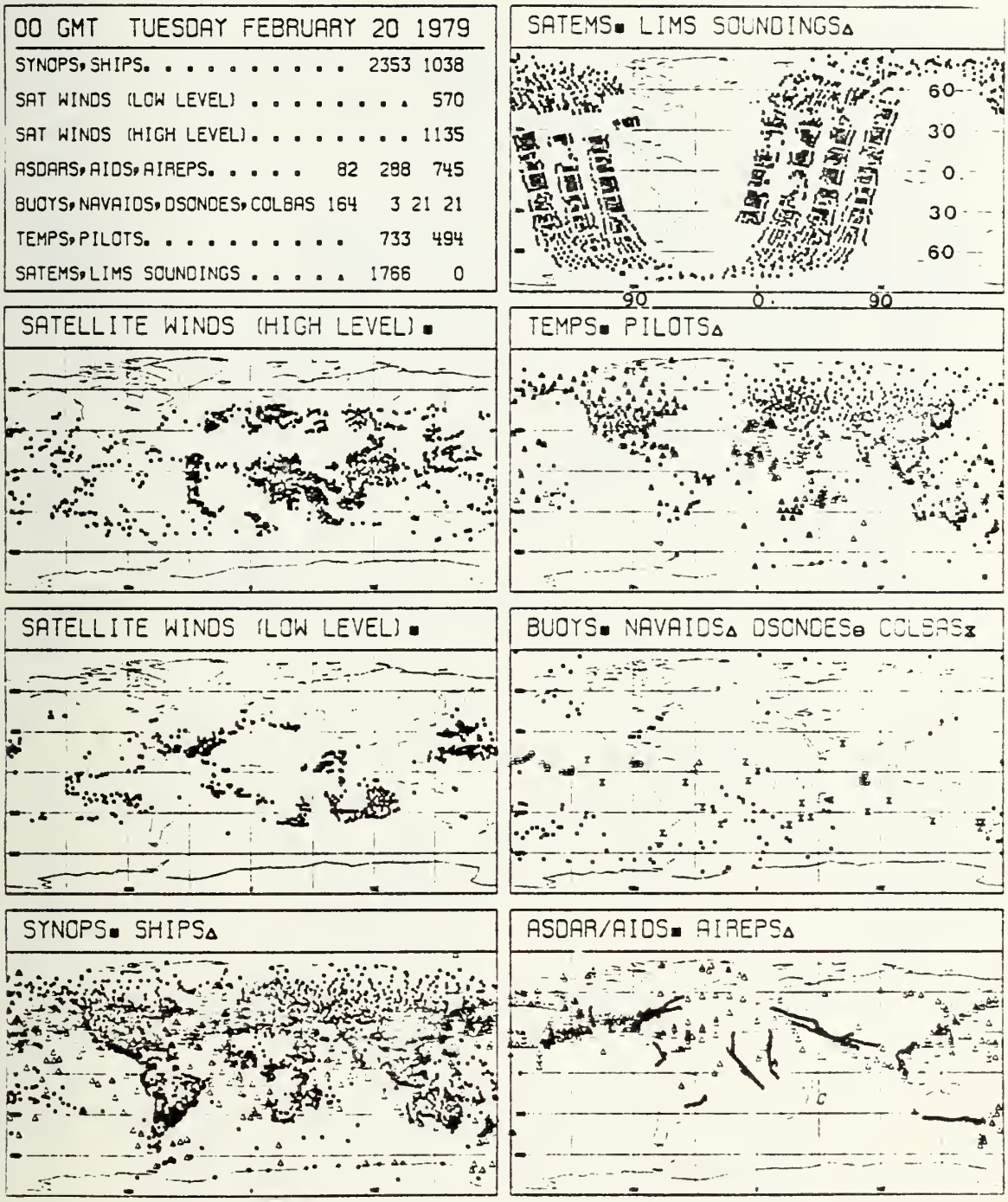

FIGURE 4. As in Figure 2 except for 0000GMT 20 February 1979.

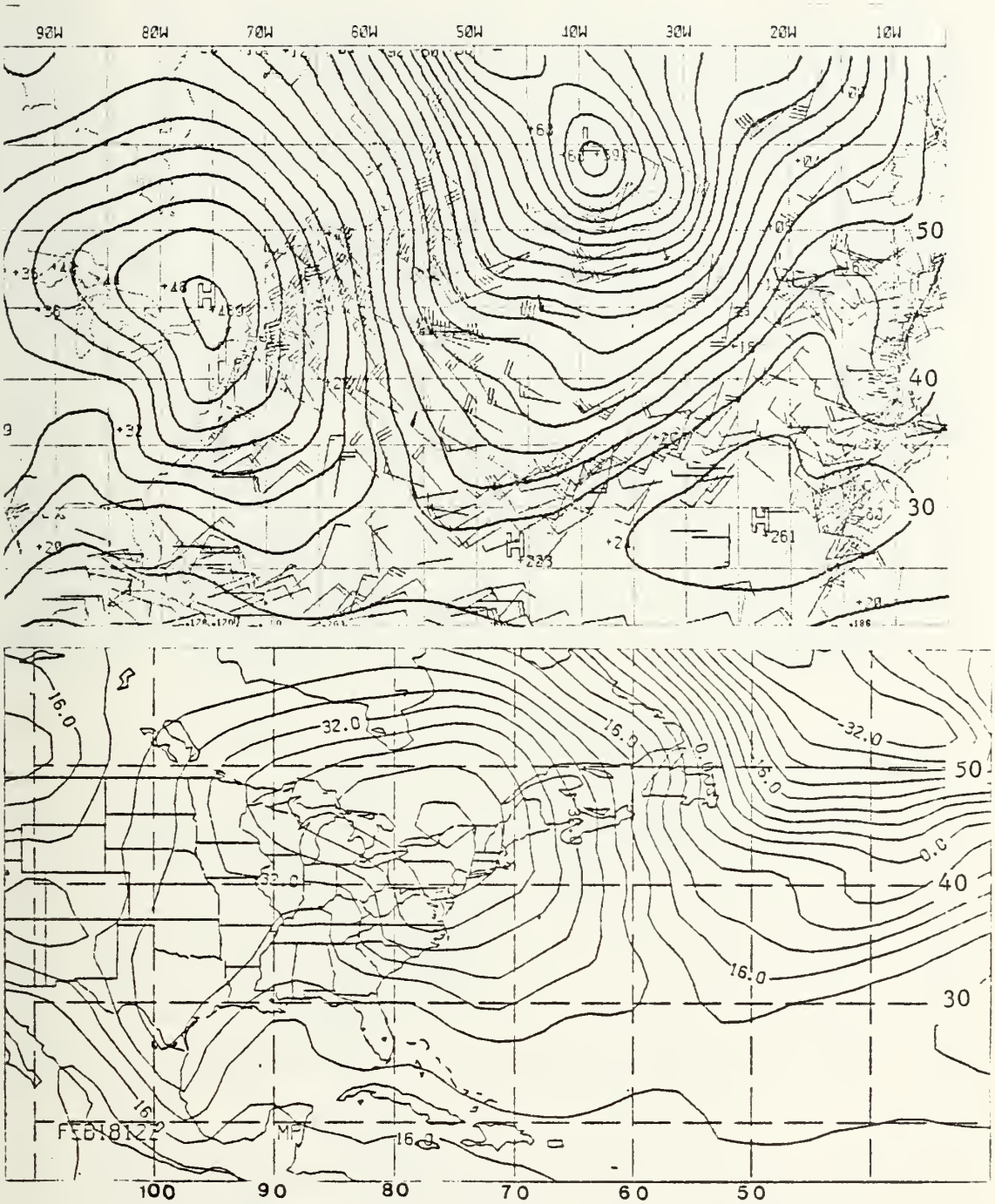

FIGURE 5. FNOC and FGGE surface pressure fields on 18 February 1979 at 1200GMT.

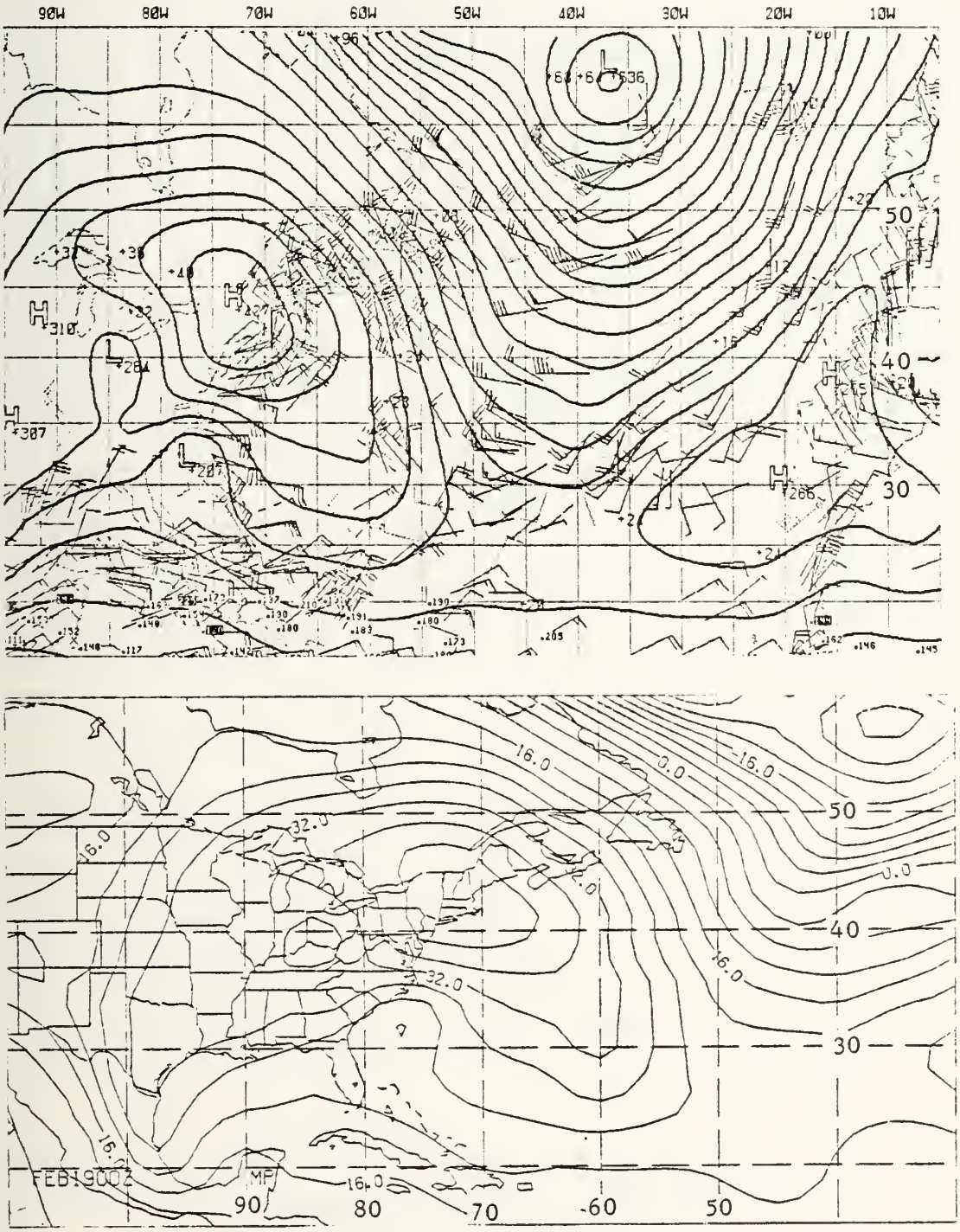

FIGURE 6. As in Figure 5 except at 0000GMT on 19 February 1979.

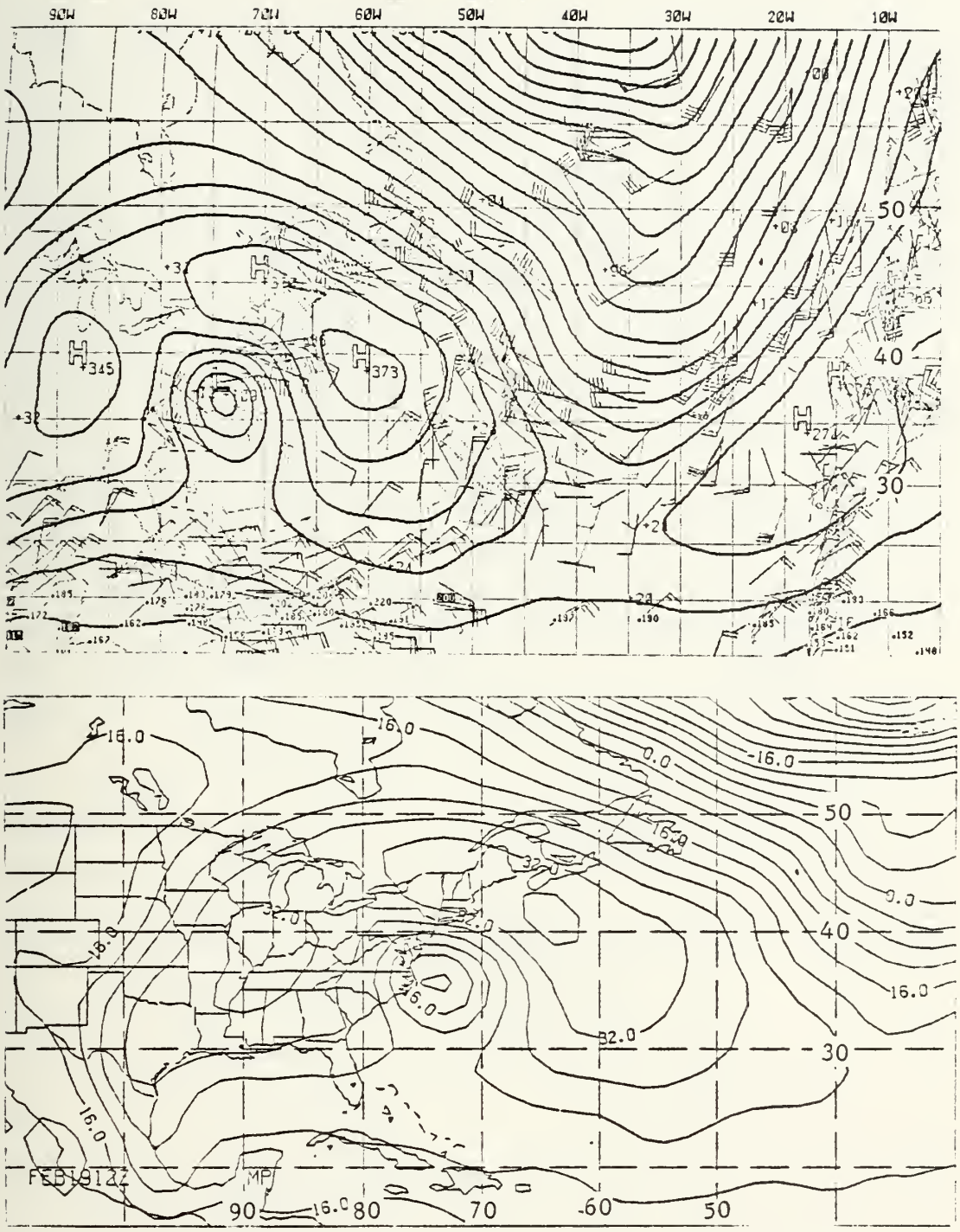

FIGURE 7. As in Figure 5 except at 1200GMT on 19 February 1979.

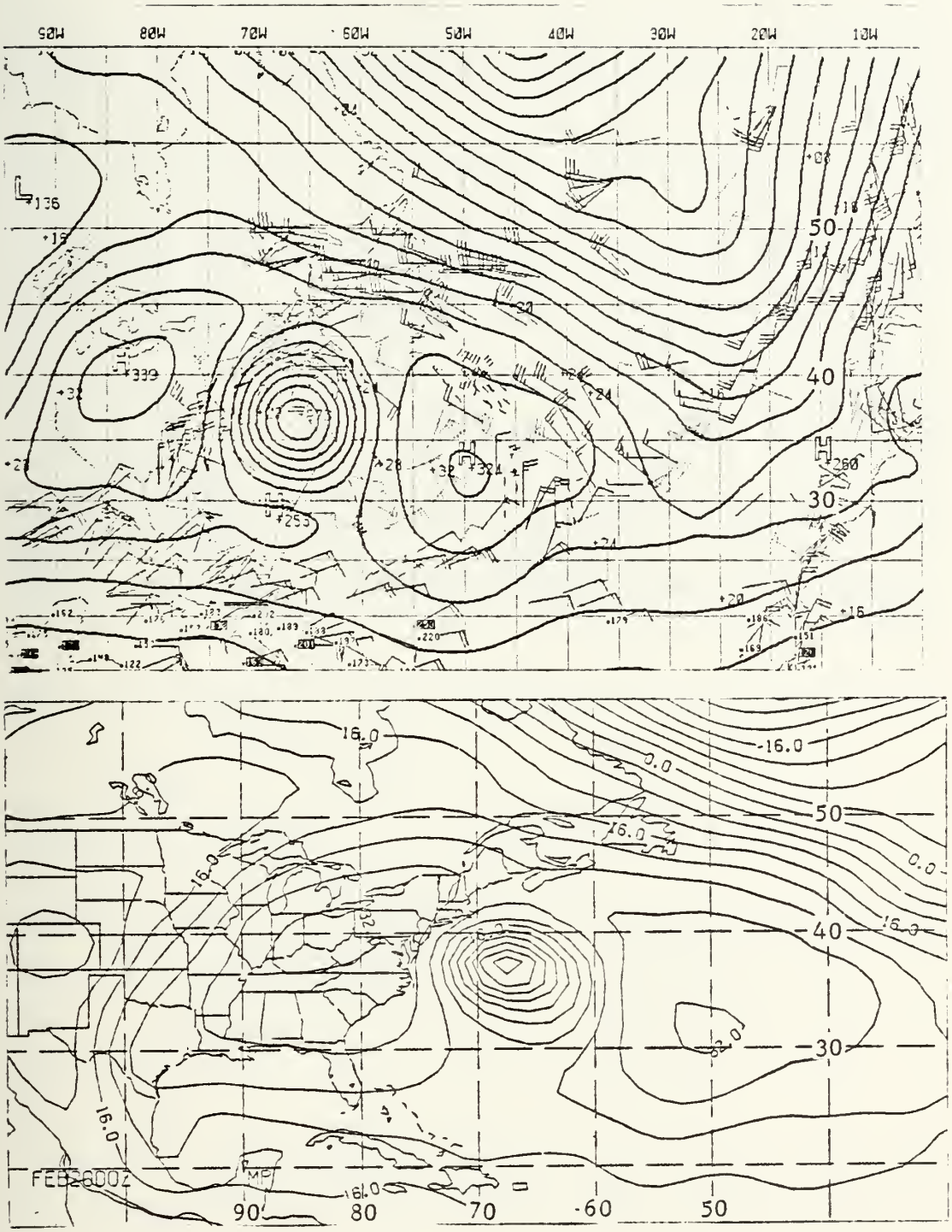

FIGURE 8. As in Figure 5 except at 0000GMT on 20 February 1979.

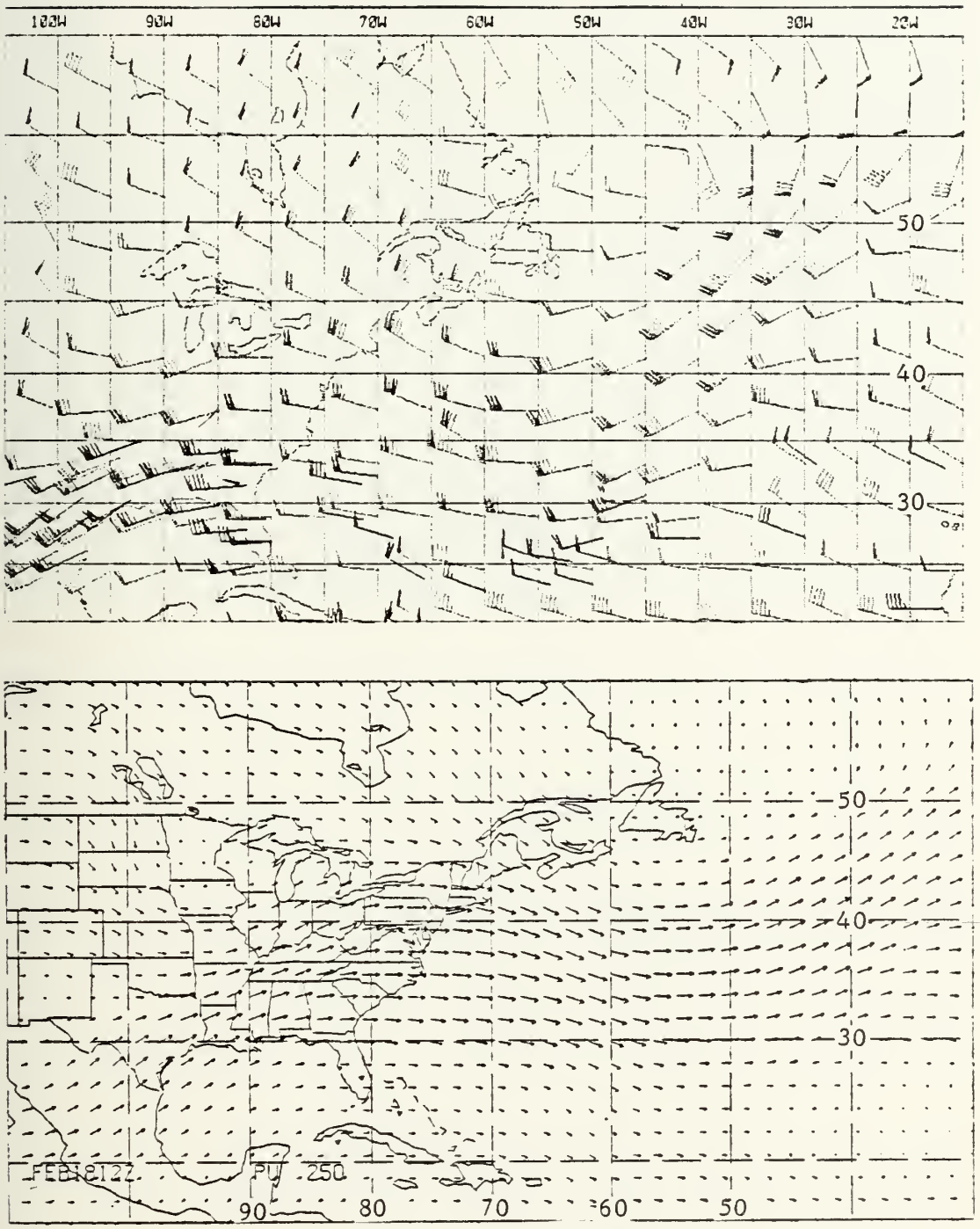

FIGURE 9. FNOC upper air analysis and the FGGE data field at the 250 mb level of 18 February 1979 at 1200GMT.

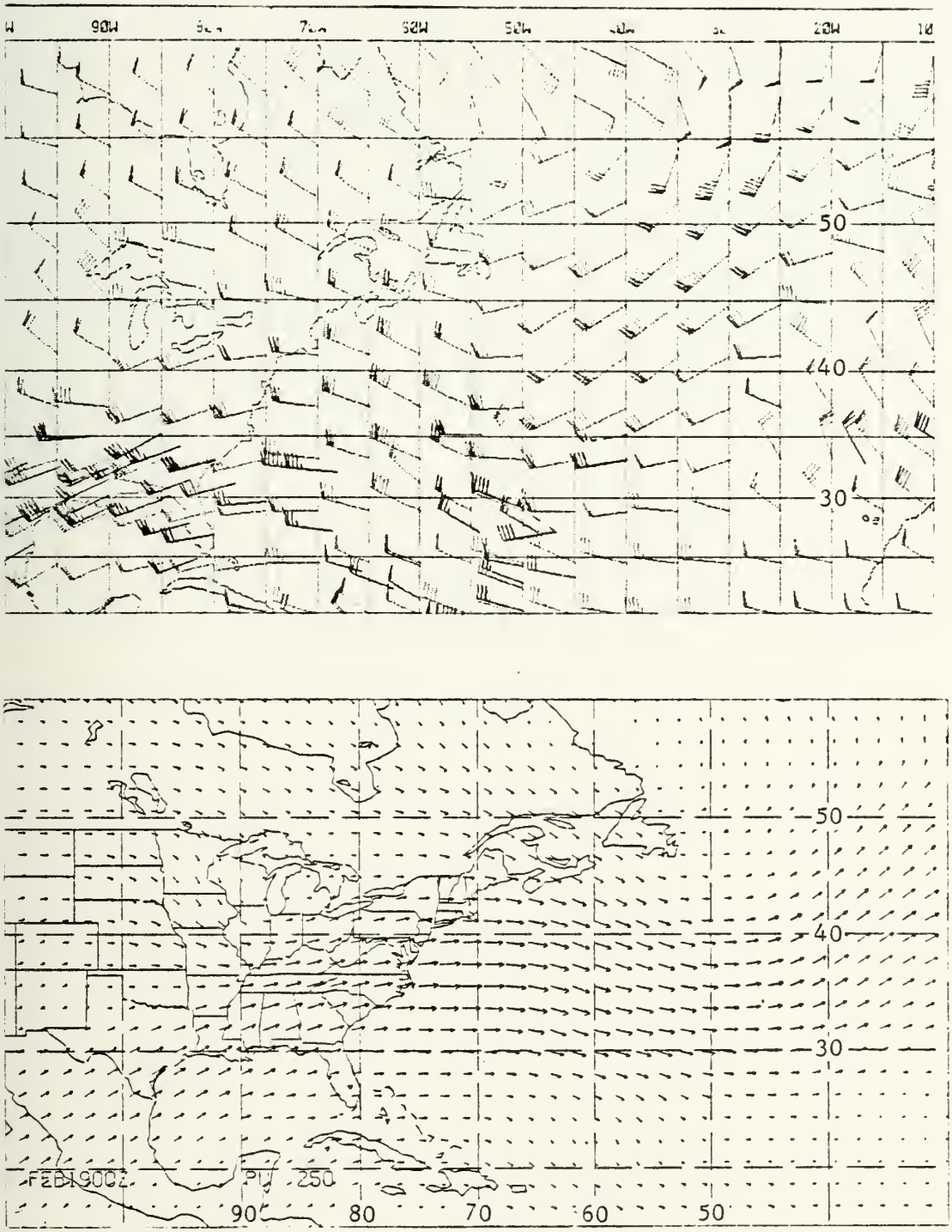

FIGURE 10. As in Figure 9 except at 0000GMT on 19 February 1979.

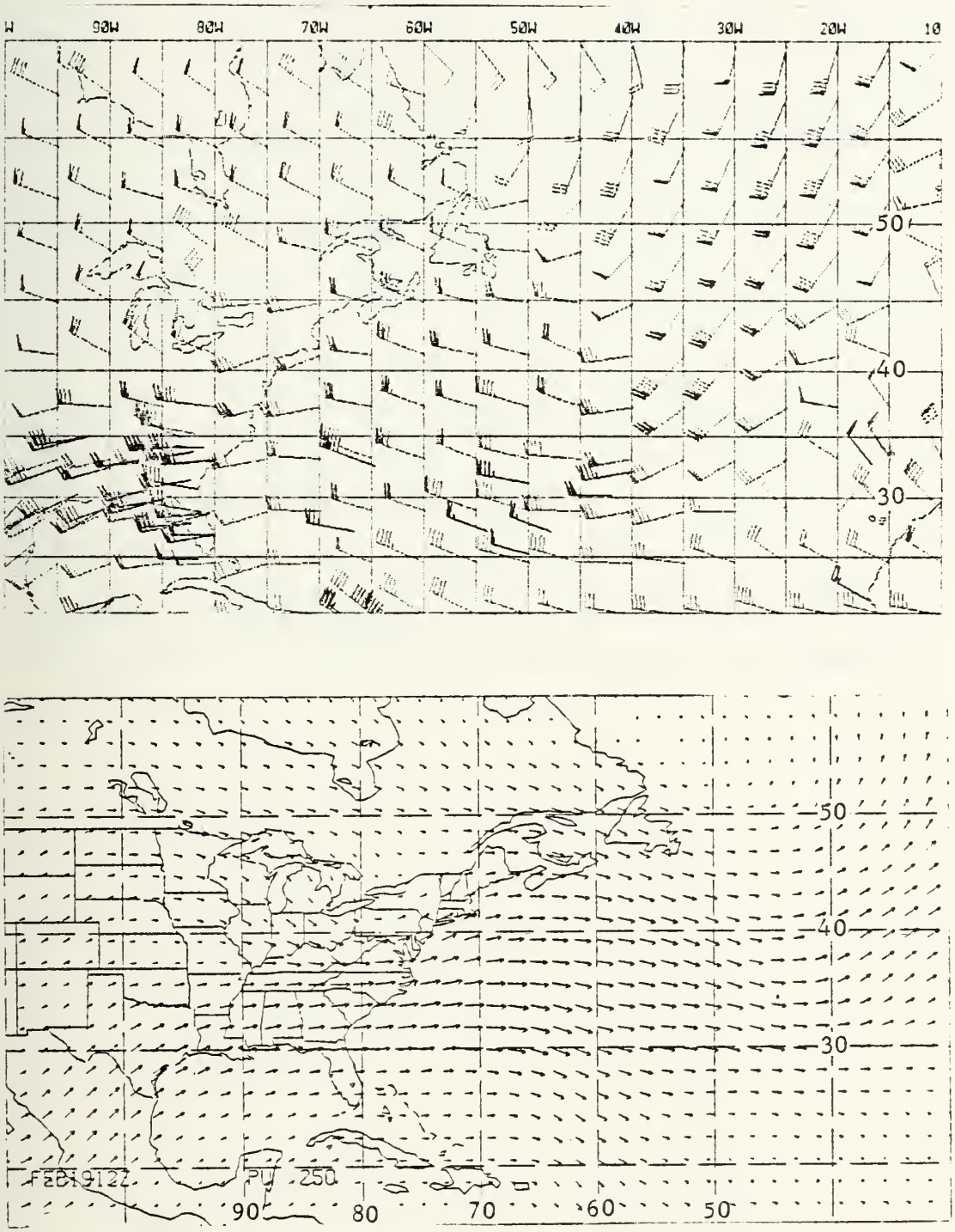

FIGURE 11. As in Figure 9 except at 1200GMT on 19 February 1979.

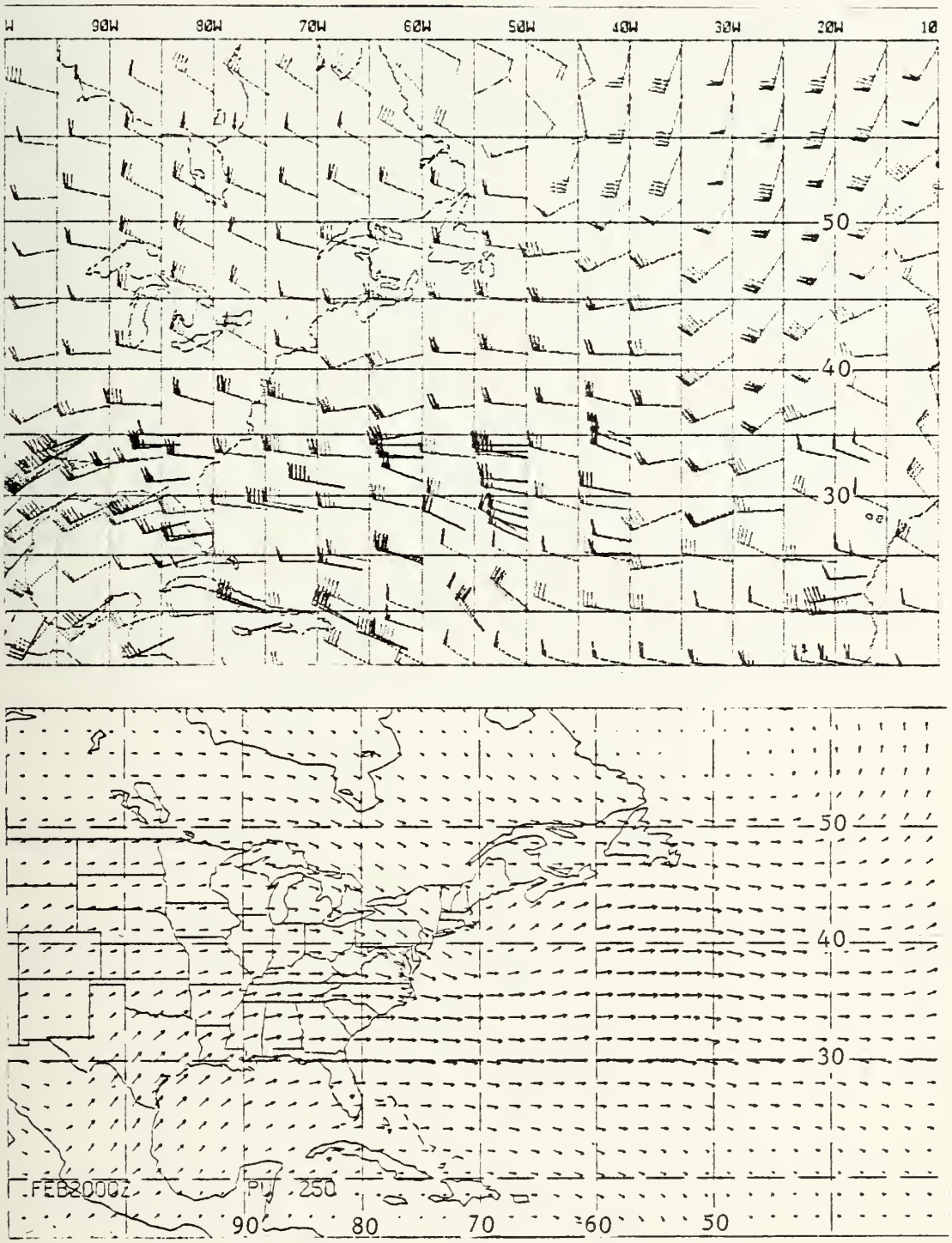

FIGURE 12. As in Figure 9 except at 0000GMT on 20 February 1979.

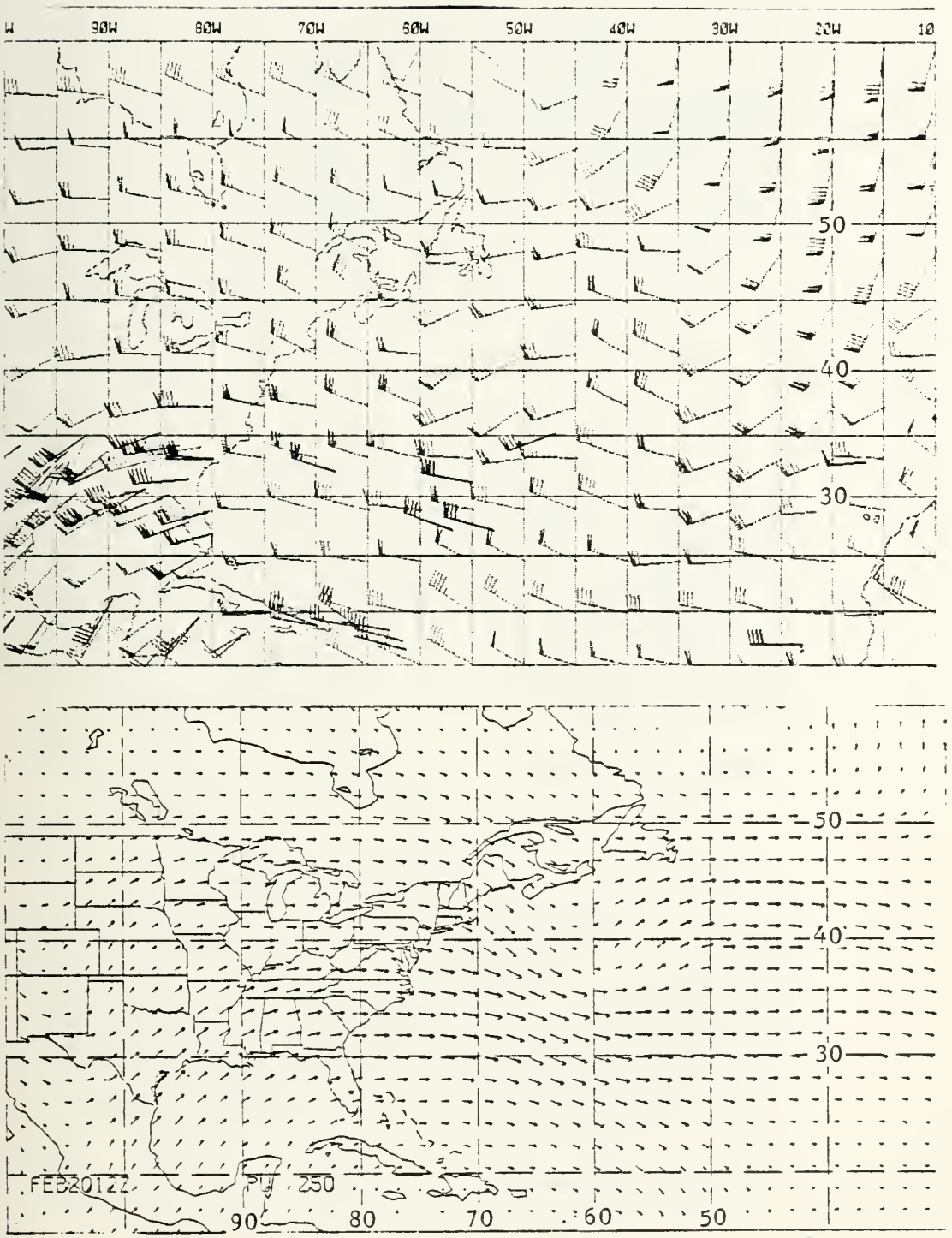

FIGURE 13. As in Figure 9 except at 1200GMT on 20 February 1979.

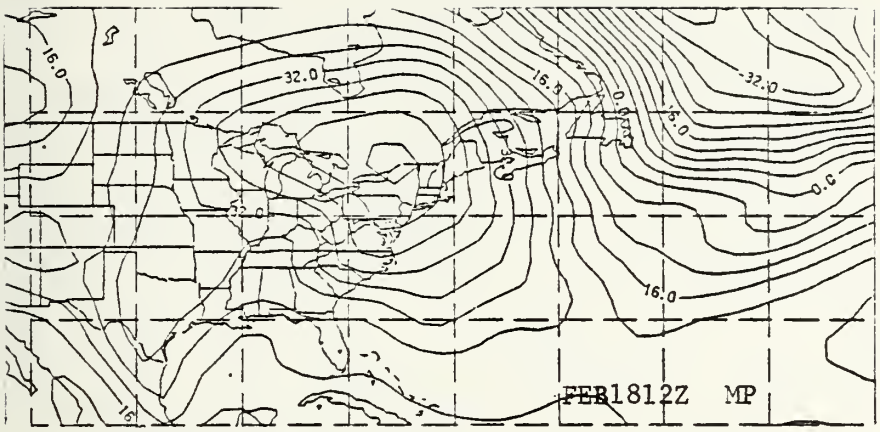

FIG. MB = MB - 1000.0

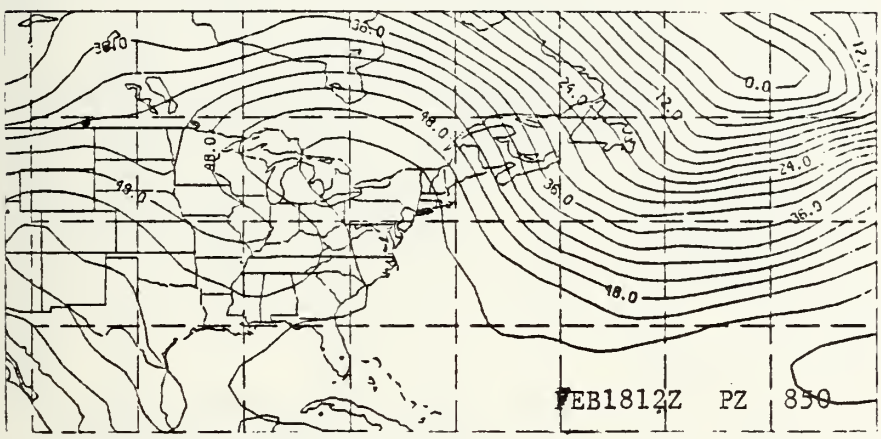

FIG. HT. = (HT.- 1000.0)/ 10.0

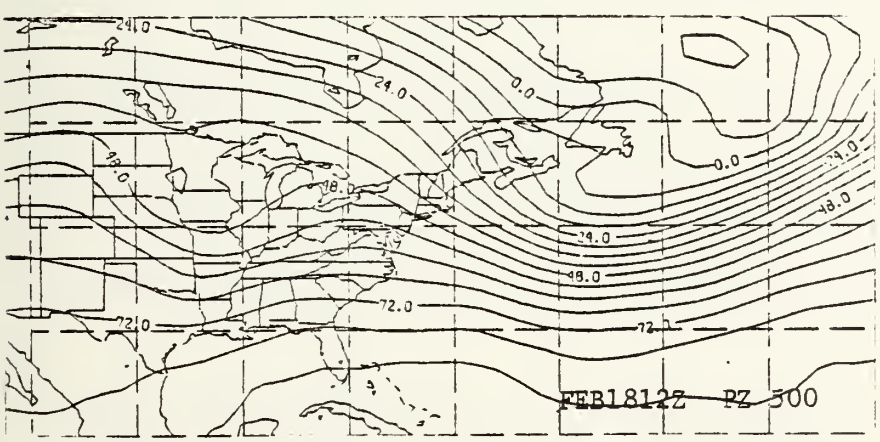

FIG. HT. = (HT. - 5000.0)/ 10.0

FIGURE 14. Surface, 850 and 500 mb charts on 18 February 1979 at 1200GMT.

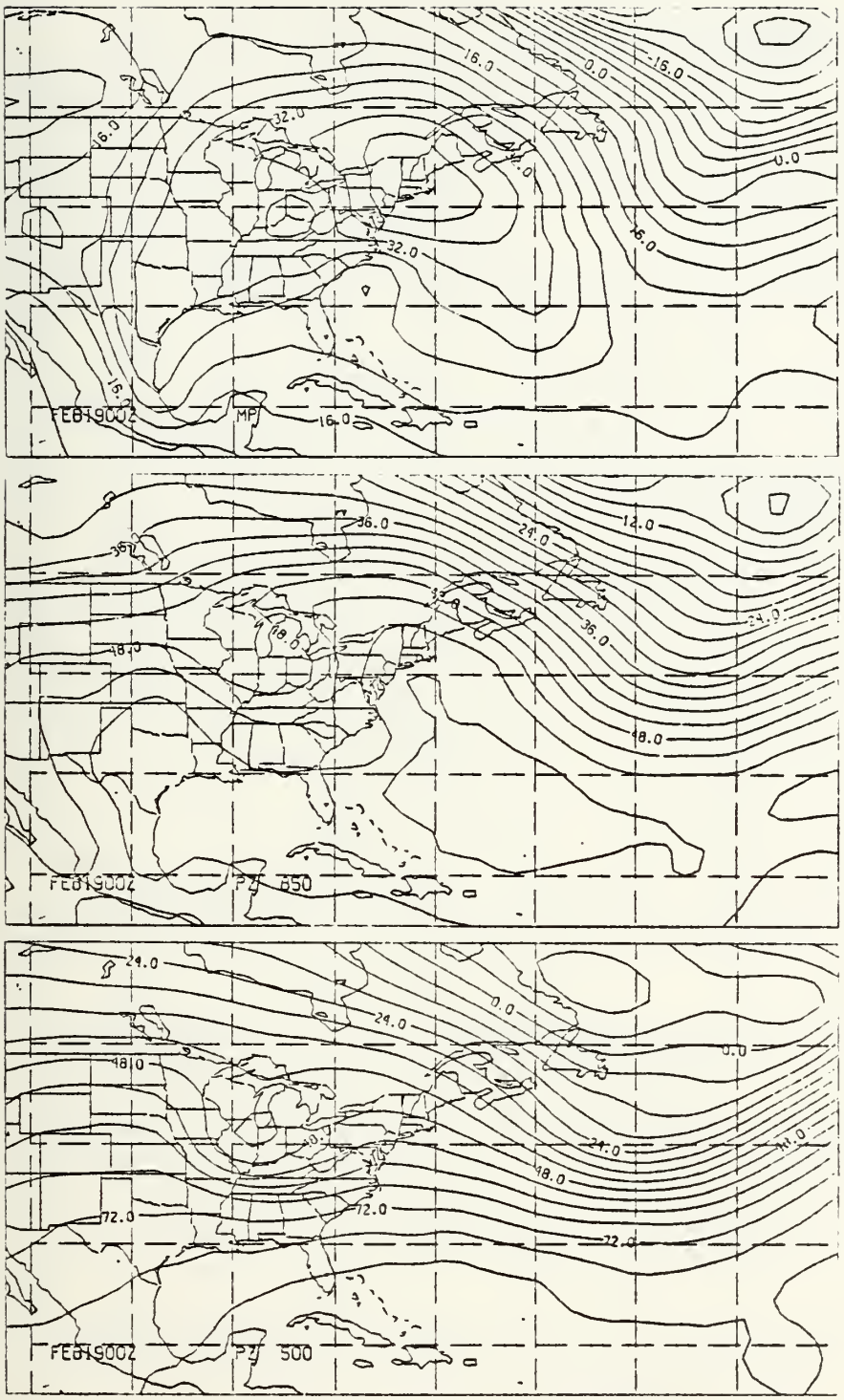

FIGURE 15. As in Figure 14 except for 0000GMT on 19 February 1979.

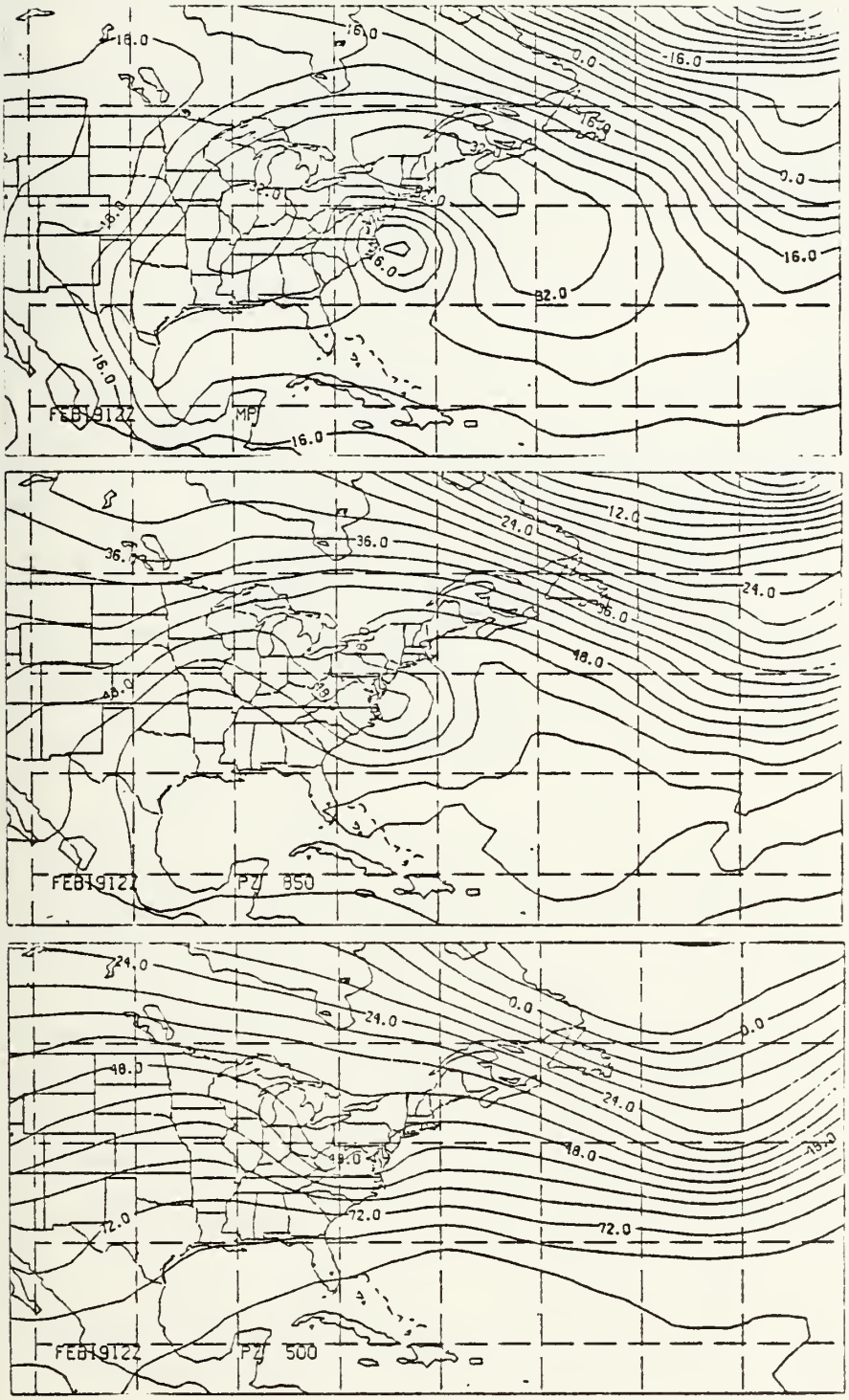

FIGURE 16. As in Figure 14 except for 1200GMT on 19 February 1979.

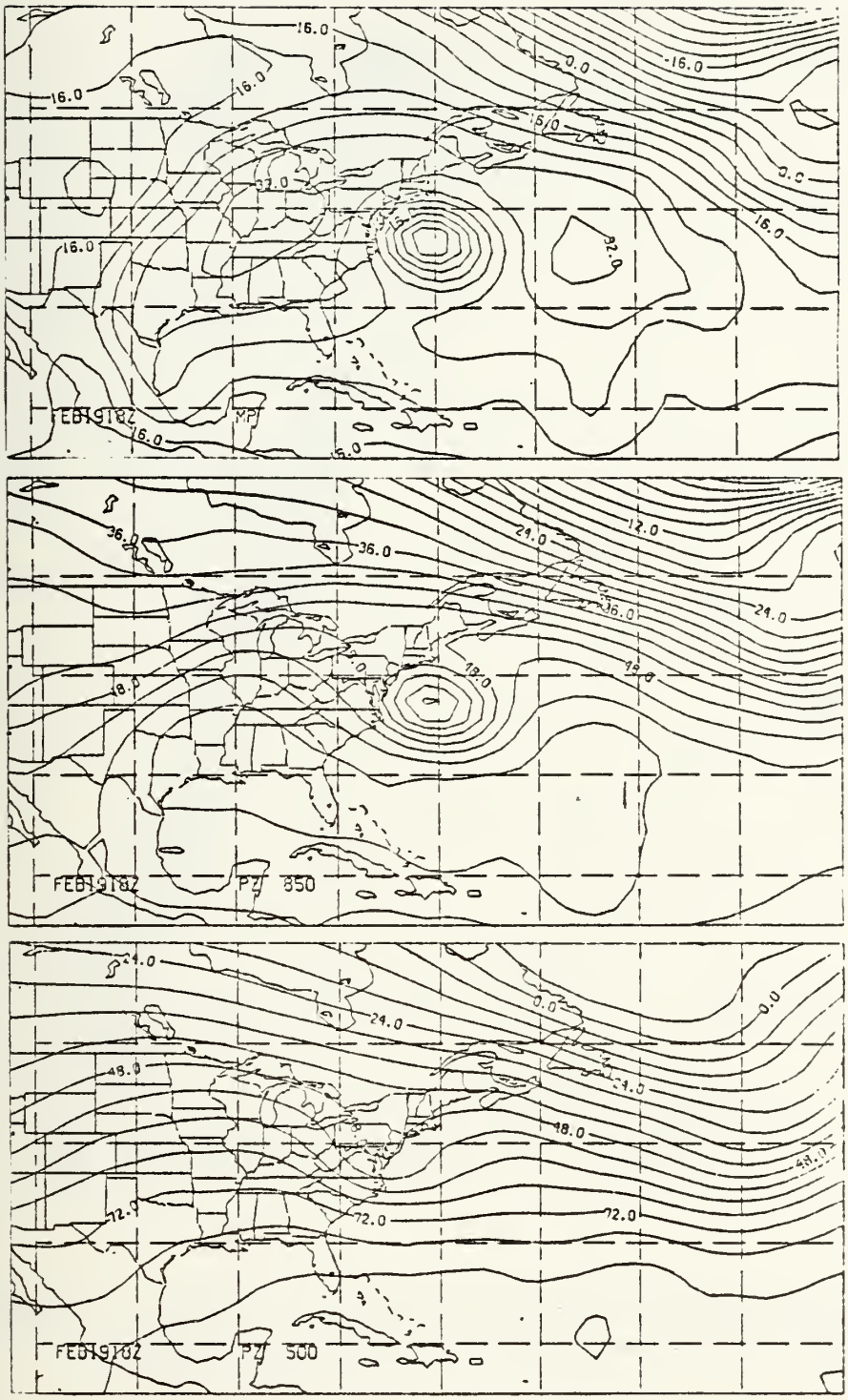

FIGURE 17. As in Figure 14 except for 1800GMT on 19 February 1979.

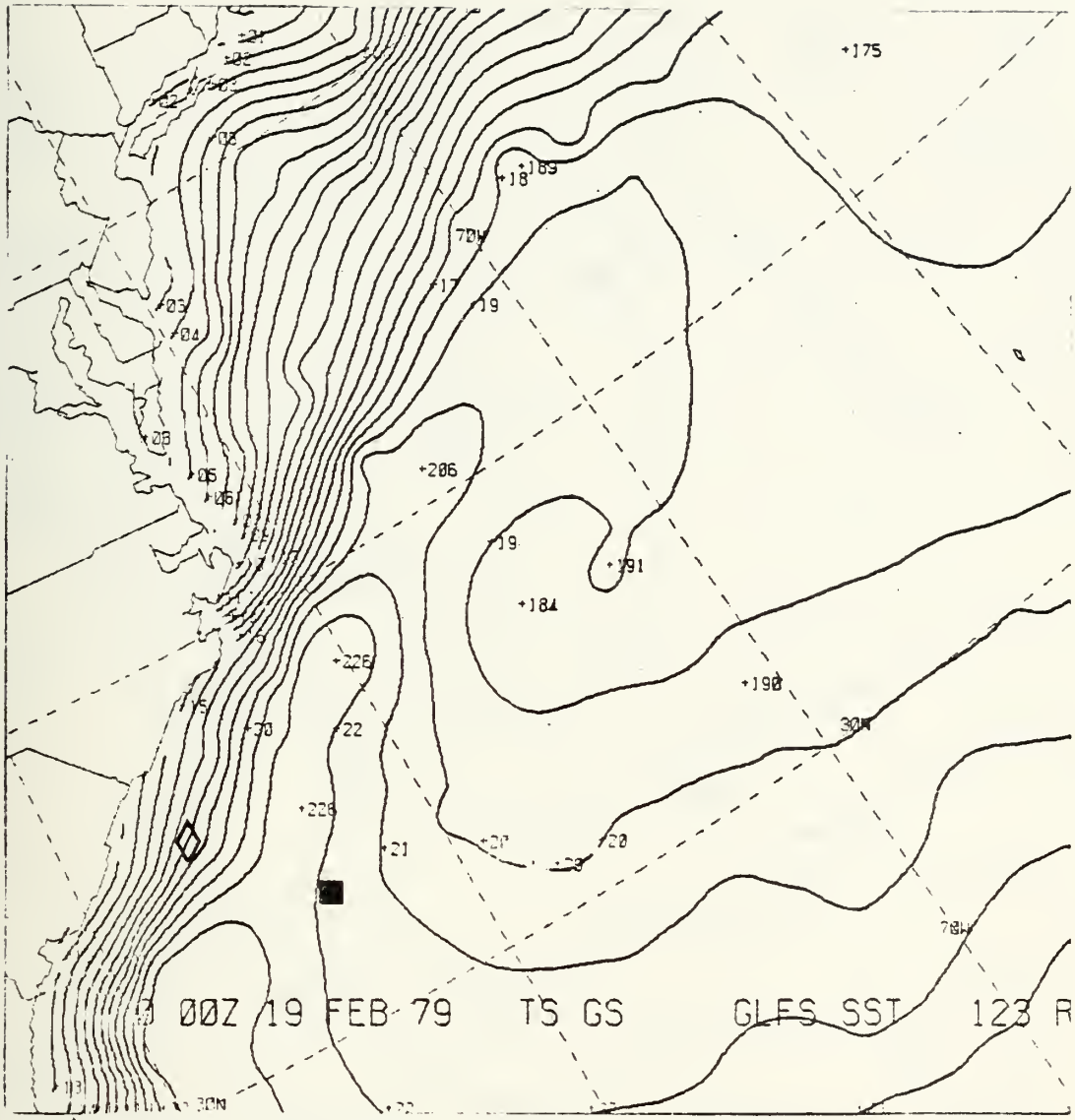

◇ Bosart's position of 19 Feb.'79 at 0000GMT.

■ FGGE position of 19 Feb.'79 at 0000GMT.

FIGURE 18. Surface low positions relative to the FNOC sea-surface temperature analysis of 19 February 1979 at 0000GMT.

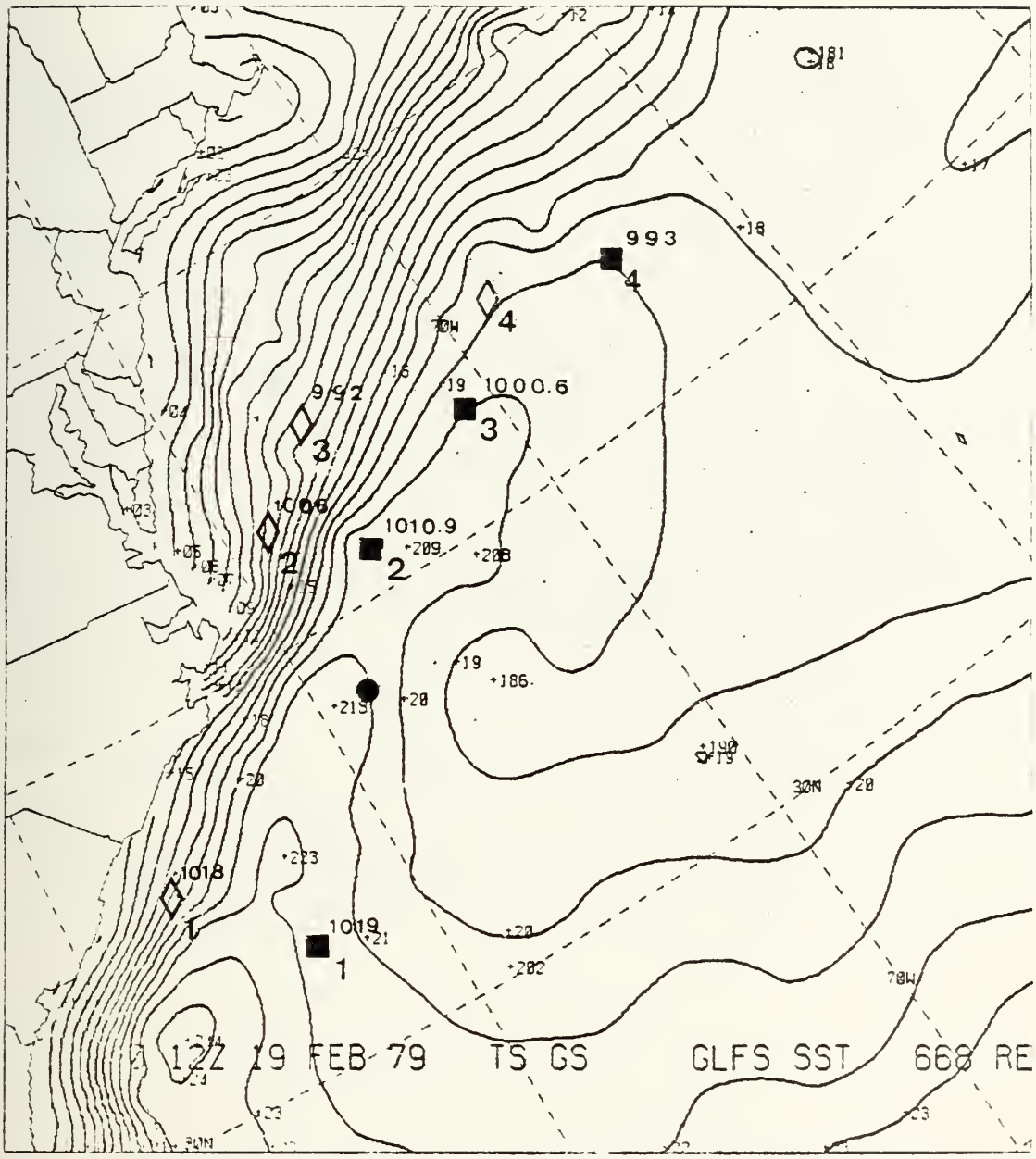

FIGURE 19. Surface low positions and central pressures relative to the FNOC sea-surface temperature analysis of 19 February 1979 at 1200GMT.

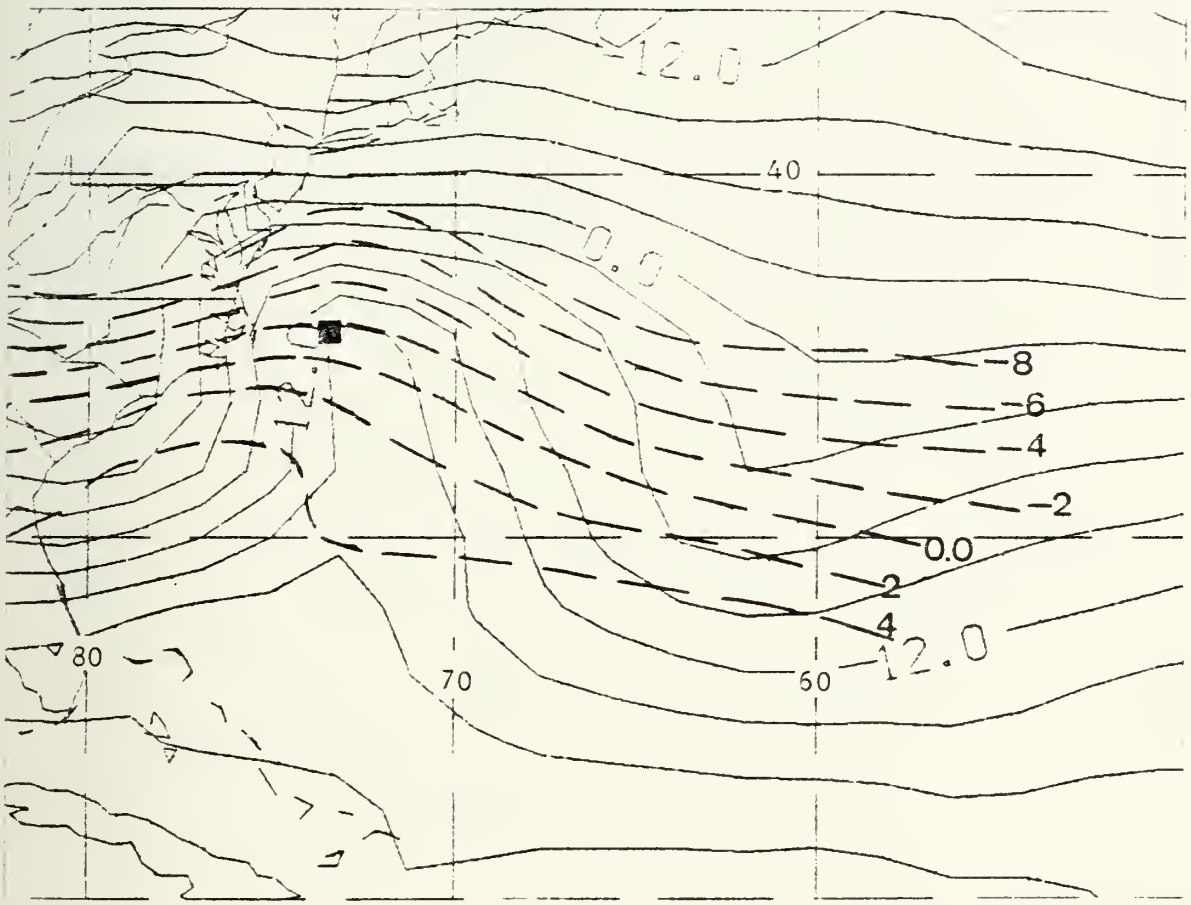

FIGURE 20. Plan-view temperature fields at 1000 and 700 mb for 19 February 1979 at 1200GMT. Black square marks the surface low location. (degrees celsius)

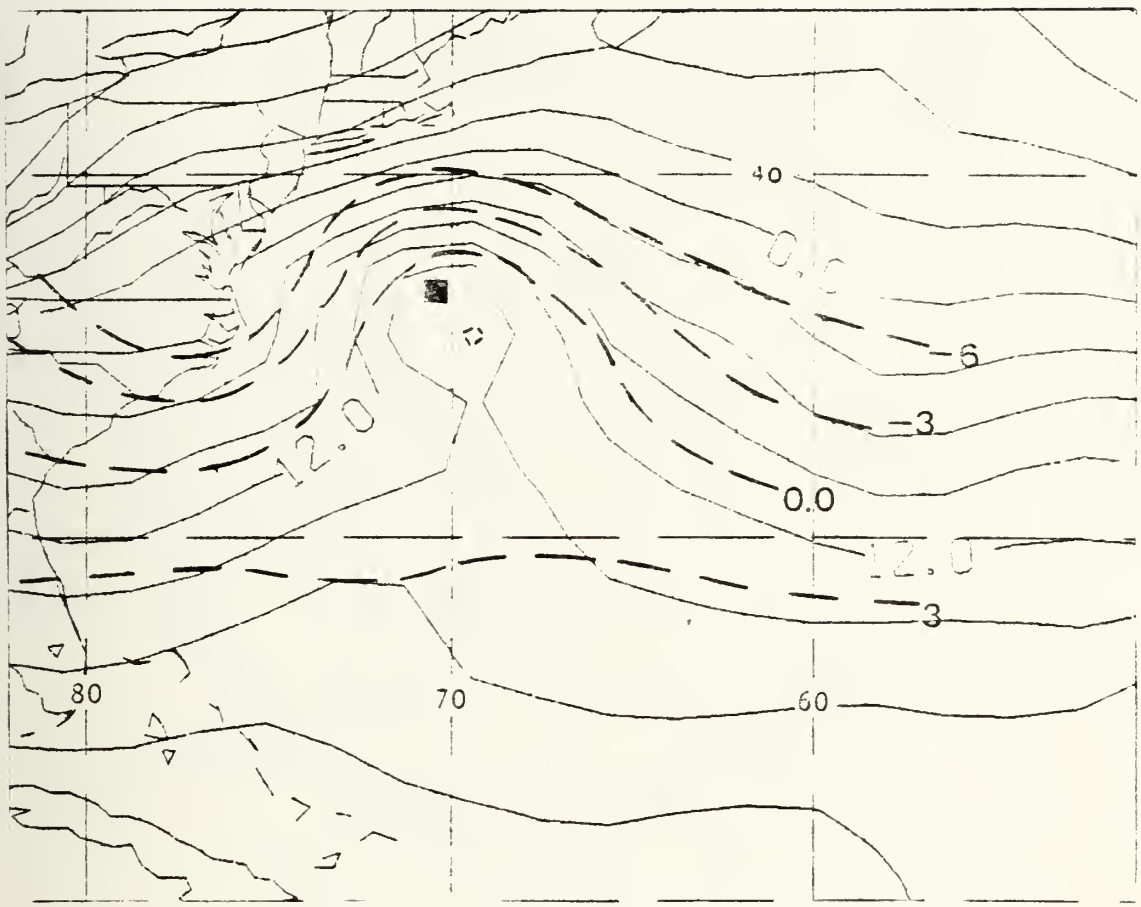

FIGURE 21. Plan-view temperature fields at 1000 and 700 mb for 19 February 1979 at 1800GMT. Black square marks the surface low location. (degrees celsius)

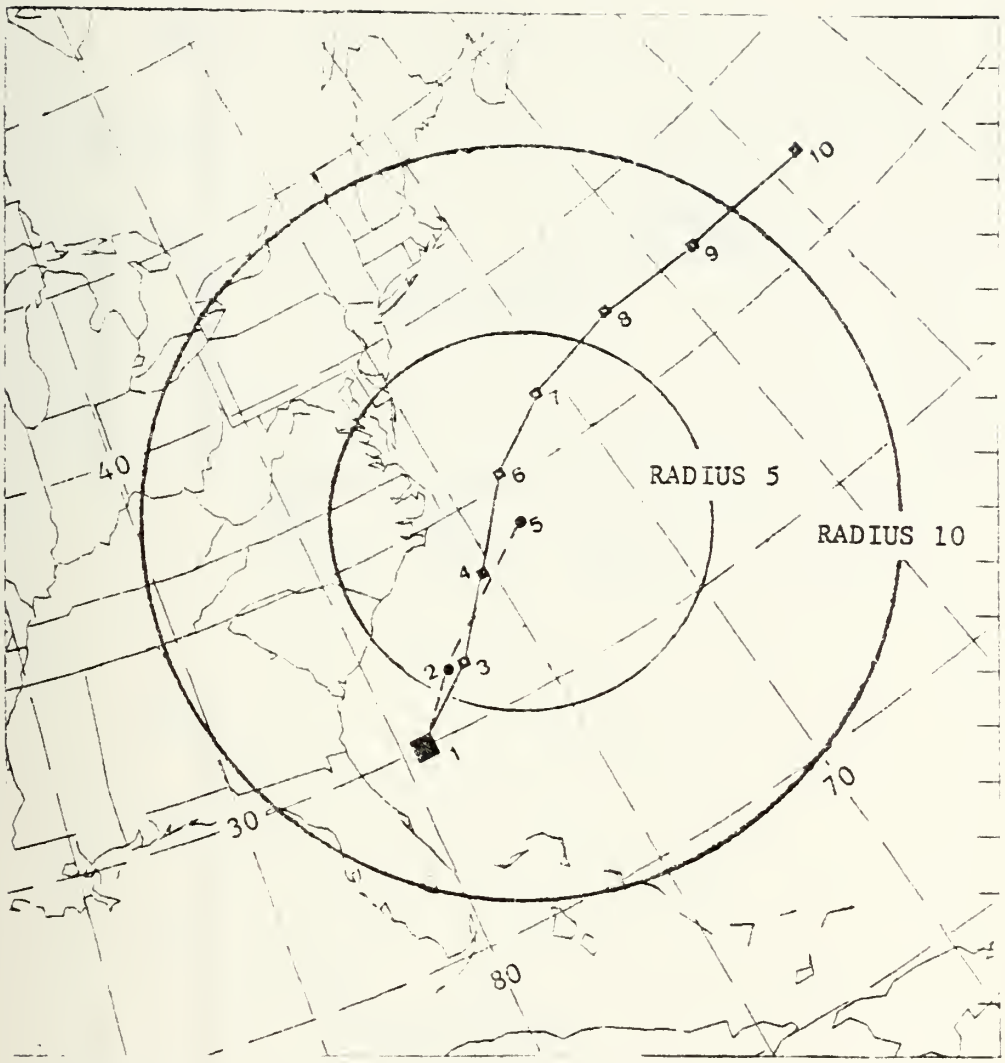

POSITION 1	L1812PA, L1812P6, L1812P12 FEB1812Z, FEB1818Z		
2	L1812P18	7	FEB1918Z
3	FEB1900Z	8	FEB2000Z
4	FEB1906Z	9	FEB2006Z
5	L1812P24	10	FEB2012Z
6	FEB1912Z		

FIGURE 22. QLD storm tracks for both the LFM and FGGE data analyses. Illustrated budget radius sizes are based on position number five. (refer to Table I for symbols)

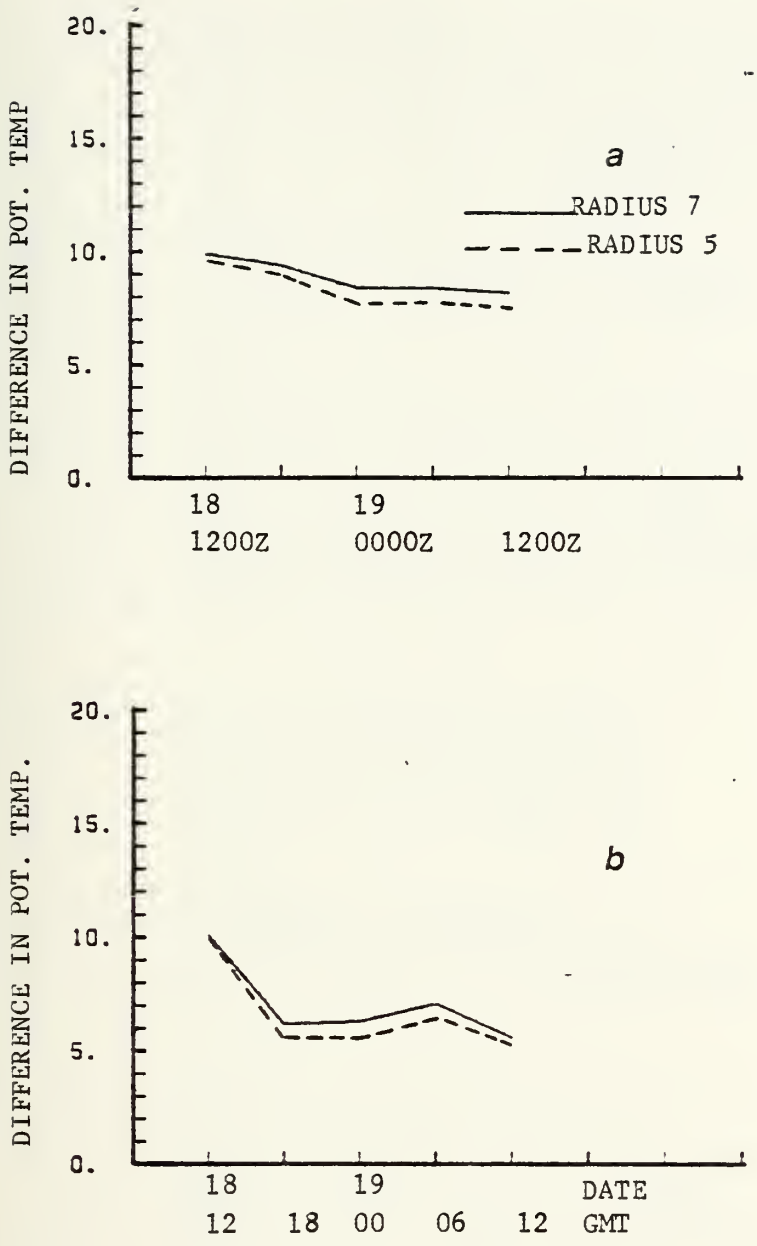

FIGURE 23. LFM potential temperature for (a) 700-850 mb and (b) 850-1000 mb for radii five (dashed) and seven (solid) plotted against time. (degrees celsius)

FIGURE 24. FGGE potential temperature for (a) 700-850 mb and (b) 850-1000 mb for radii five (dashed) and seven (solid) plotted against time. (degrees celsius)

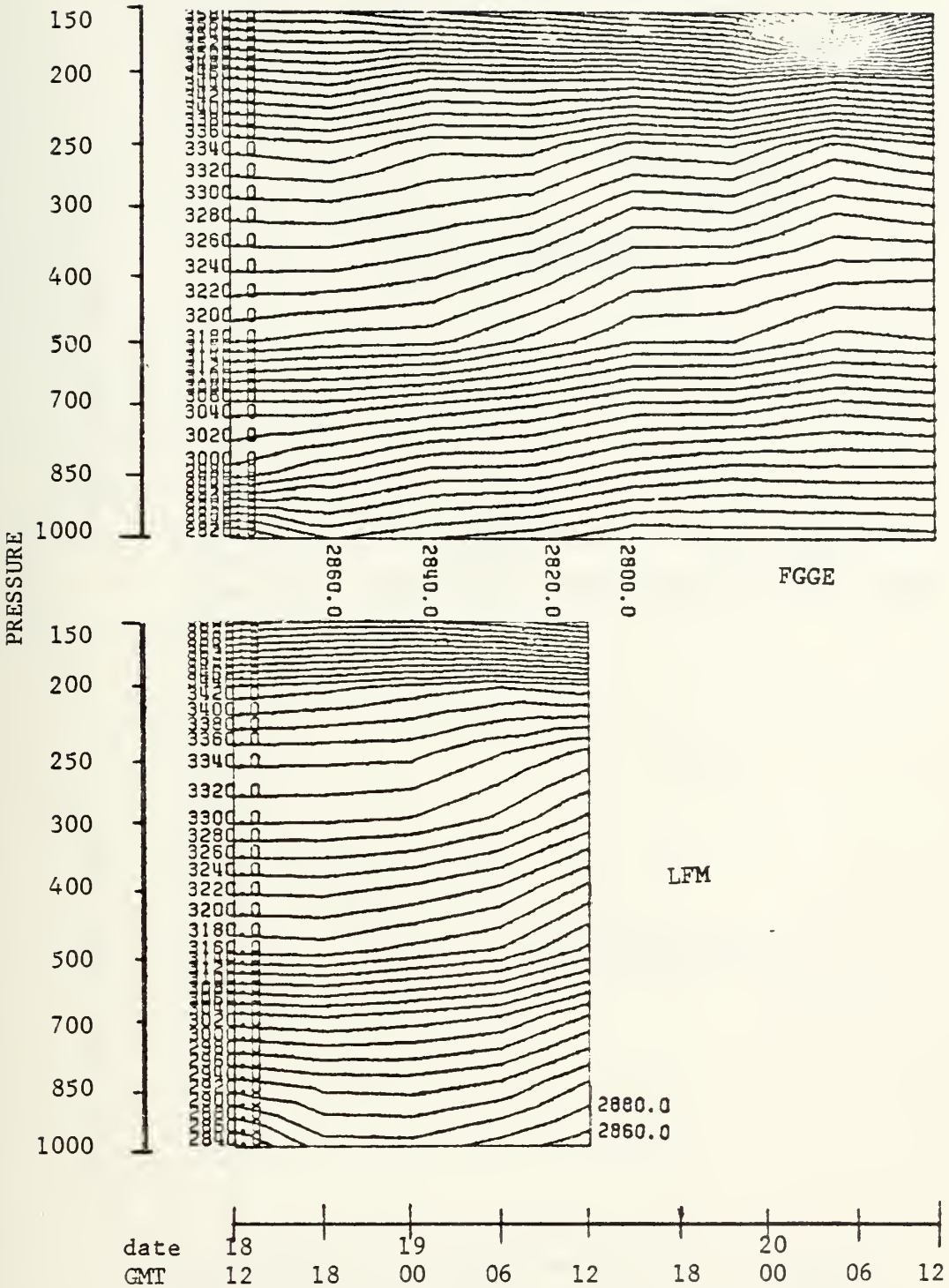

FIGURE 25. Time evolution of FGGE and LFM potential temperature (°K) fields of radius six. (value/10 = degrees Kelvin)

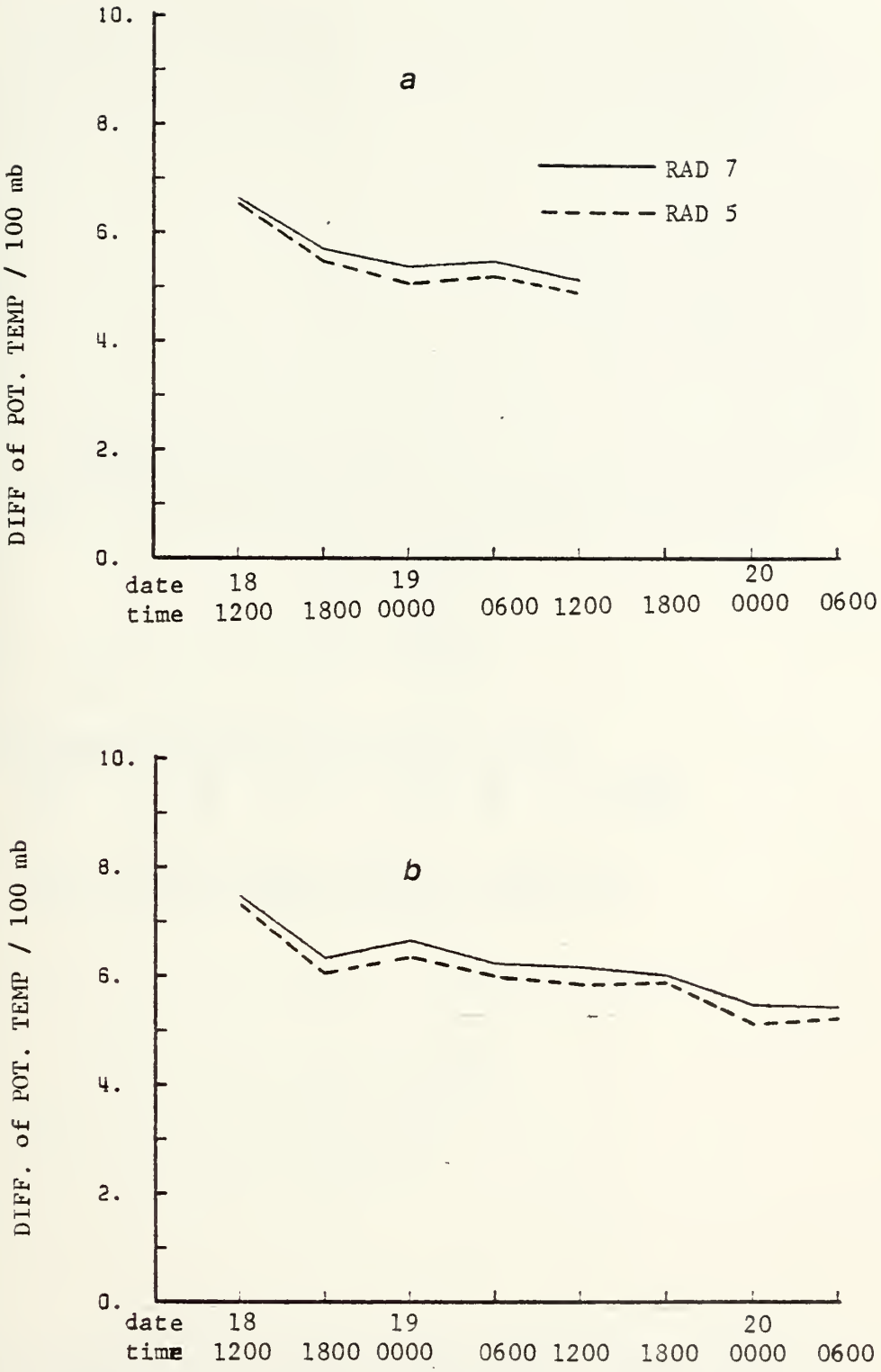

FIGURE 26. Difference in potential temperature (°K per 100 mbs) between 1000 and 500 mb at radii five (dashed) and seven (solid) from (a) LFM analysis and (b) FGGE analysis.

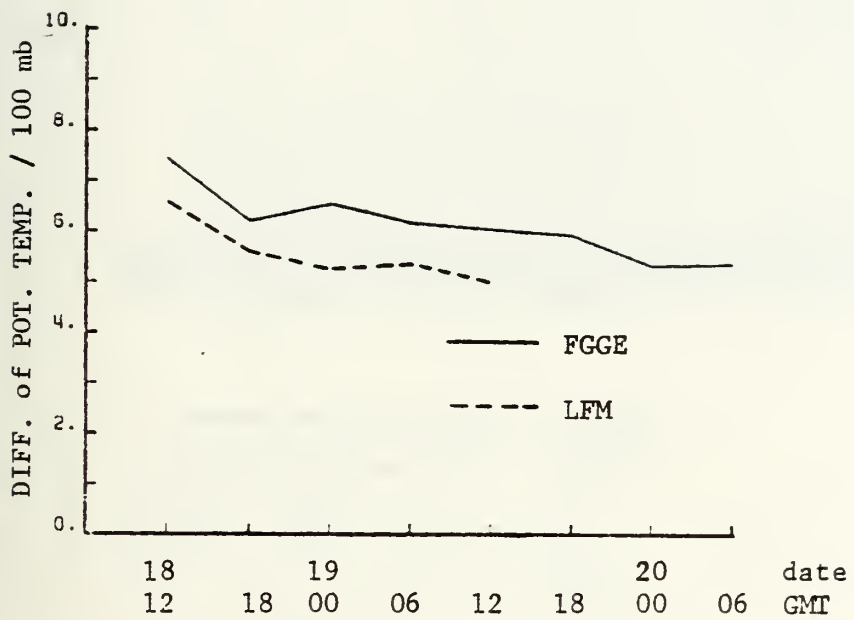

FIGURE 27. Difference in potential temperature (°K per 100 mbs) between 1000 and 500 mb with both the LFM (dashed) and FGGE (solid) data for radius six.

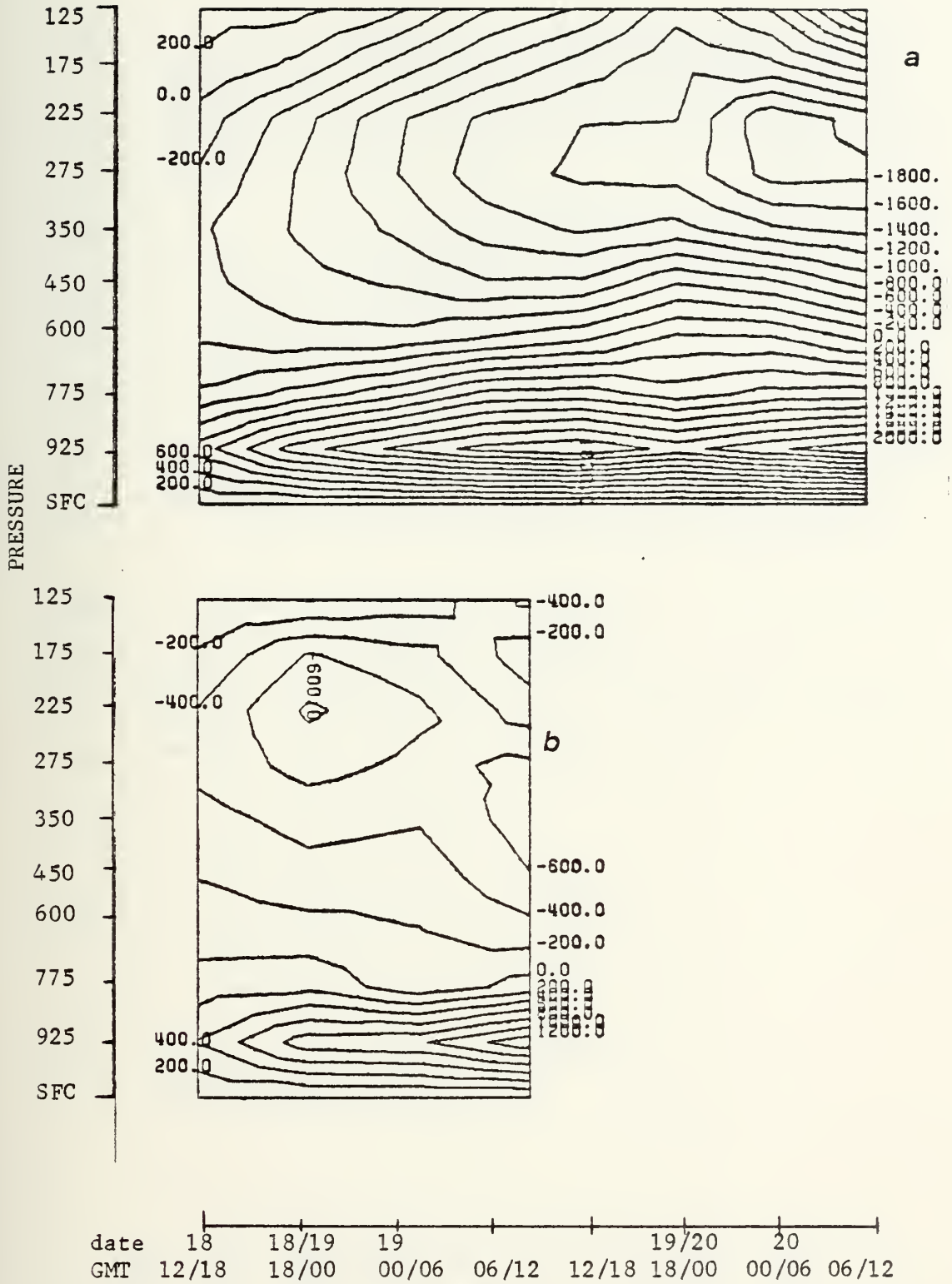

FIGURE 28. Time series of (a) FGGE and (b) LFM lateral mass transport at radius six.

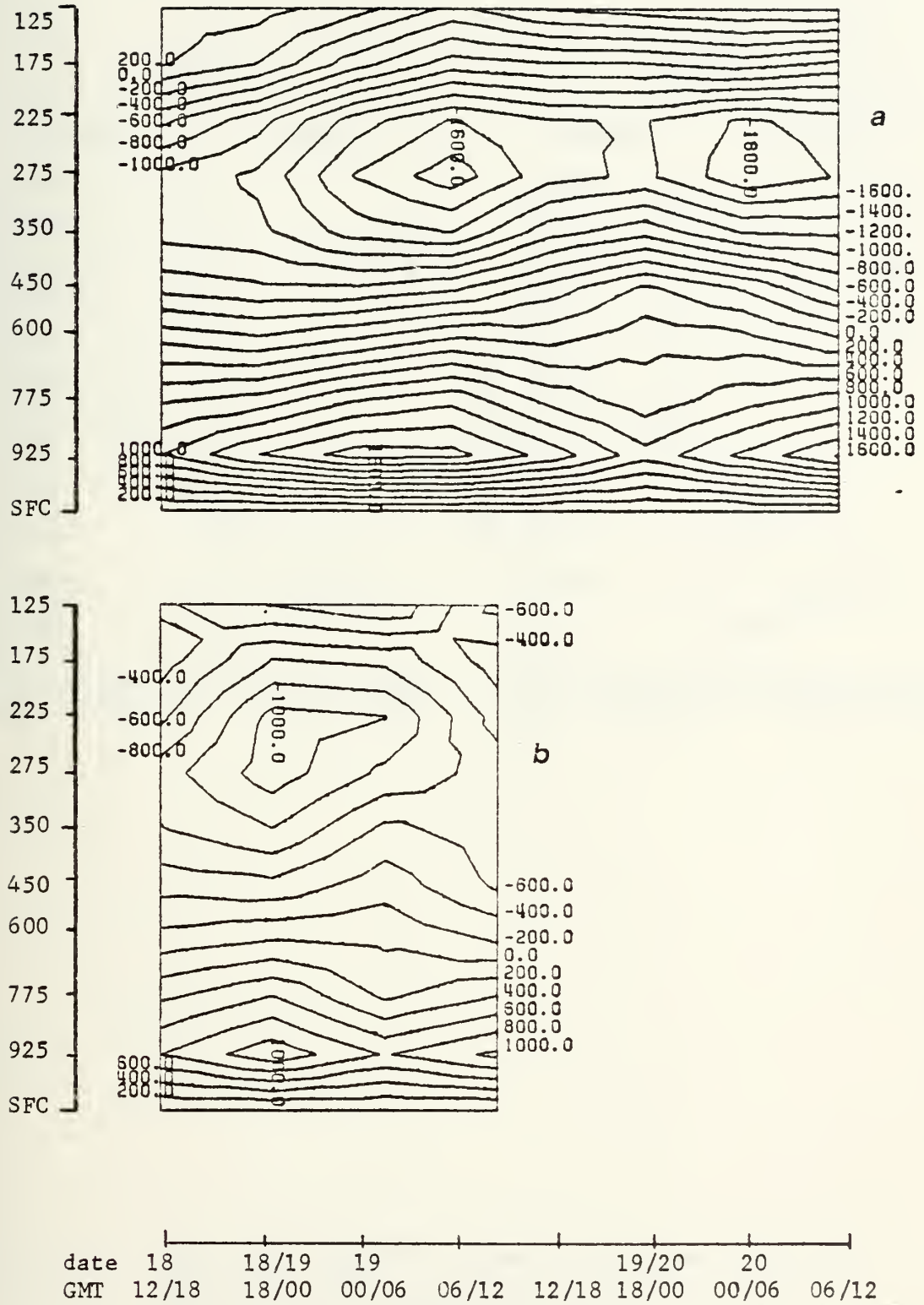

FIGURE 29. Time series of (a) FGGE and (b) LFM lateral mass transport at radius nine.

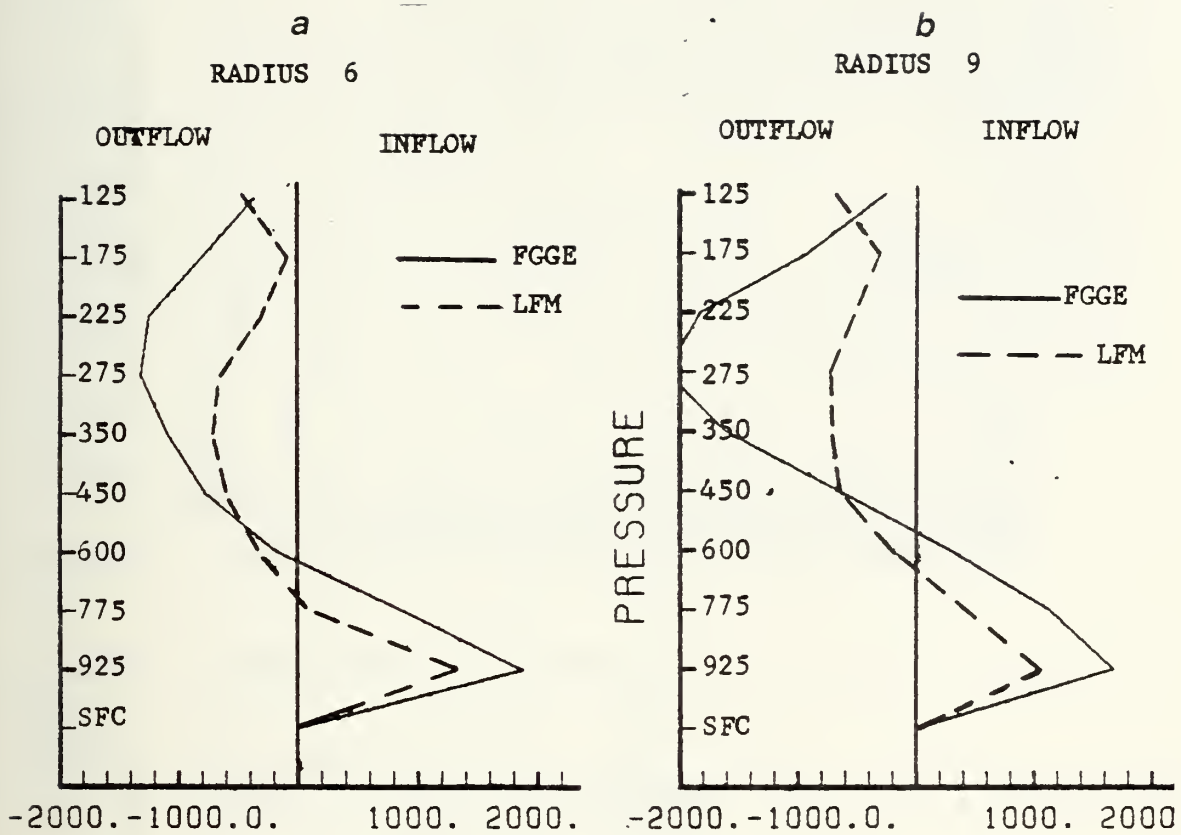

FIGURE 30. FGGE (solid) and LFM (dashed) lateral mass transport profiles for radius (a) six and (b) nine. (value x 10**10 = grams/sec/100 mb)

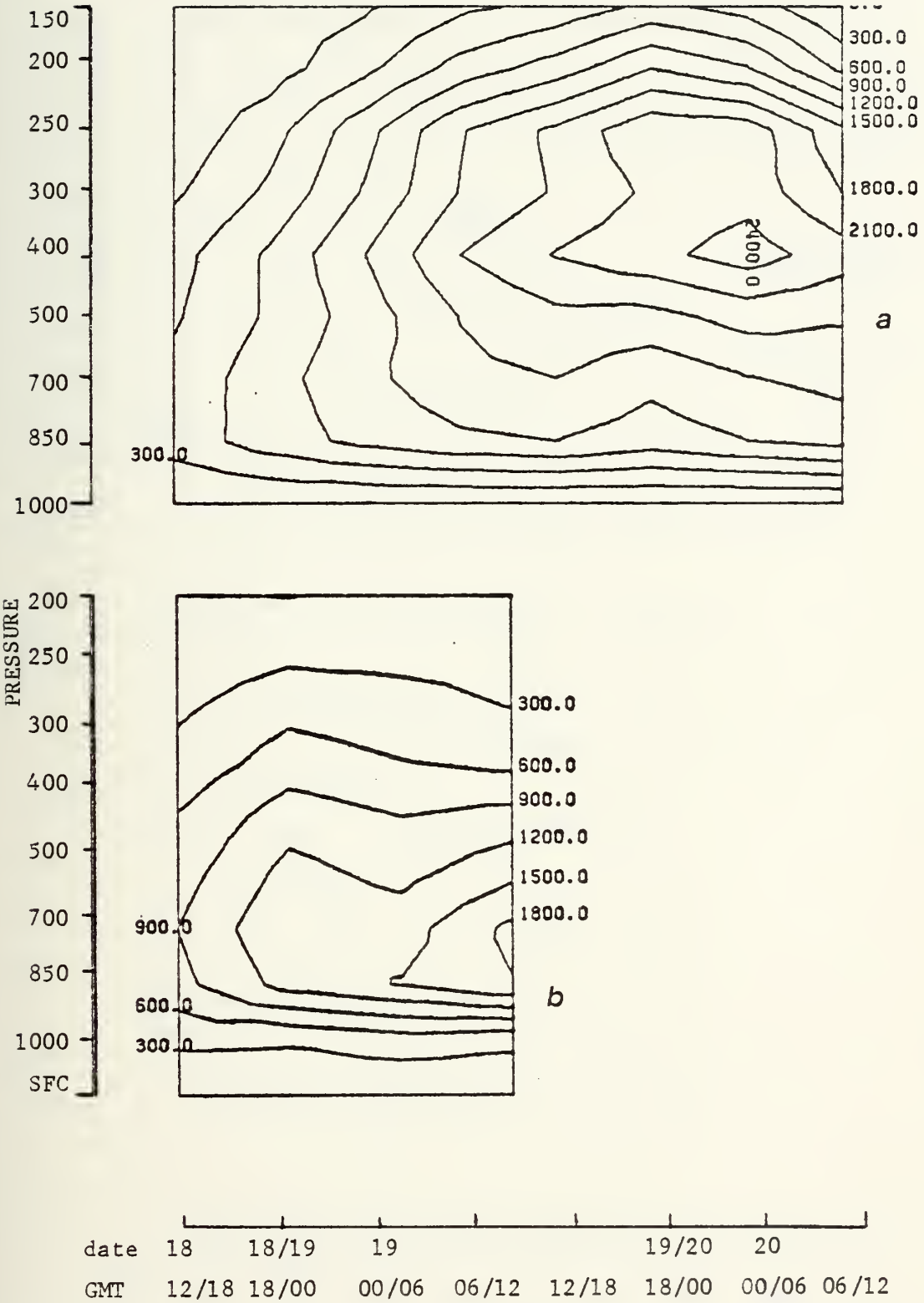

FIGURE 31. Time series of (a) FGGE and (b) LFM vertical velocity fields of radius six. (value/1000 = mb/sec)

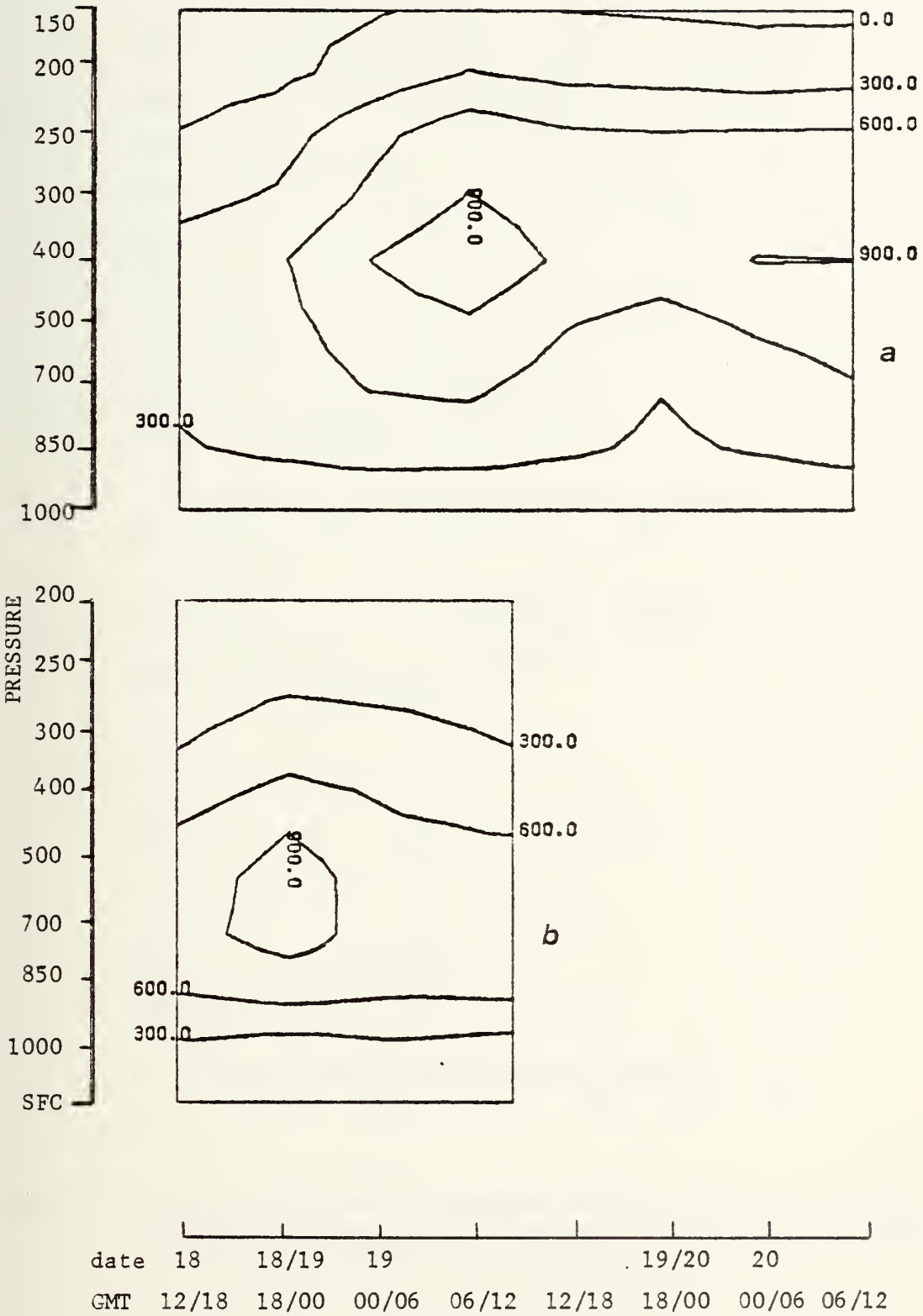

FIGURE 32. Time series of (a) FGGE and (b) LFM vertical velocity fields of radius nine. (value/1000 = mb/sec)

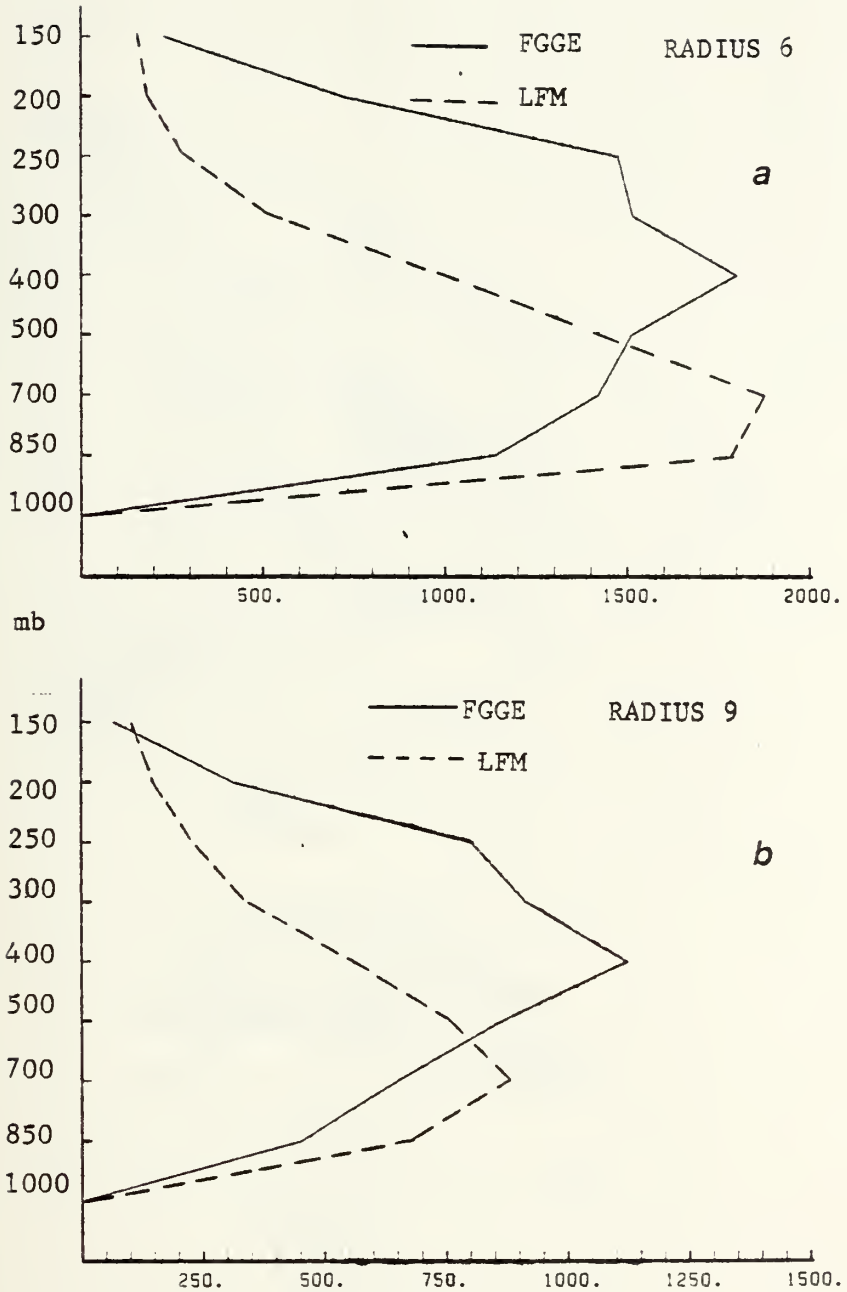

FIGURE 33. FGGE (solid) and LFM (dashed) vertical velocity profiles of radii (a) six and (b) nine for period 0600 to 1200GMT on 19 February 1979. (value/1000 = mb/sec)

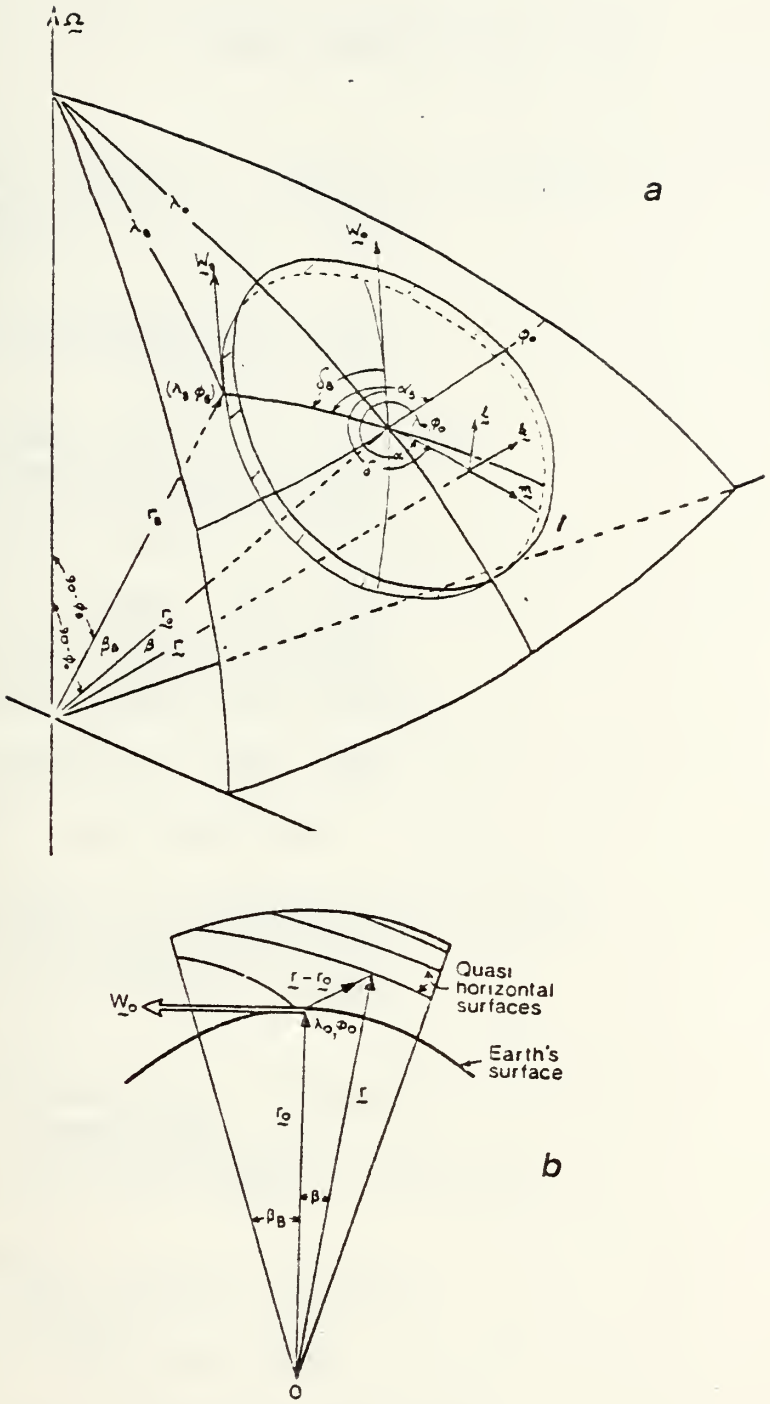

FIGURE 34. (a) Storm budget volume coordinate system and (b) a storm volume cross section (adopted from Wash, 1978).

INITIAL DISTRIBUTION LIST

		No. Copies
1.	Defense Technical Information Center Cameron Station Alexandria, Virginia 22314	2
2.	Library, Code 0142 Naval Postgraduate School Monterey, California 93940	2
3.	Department Chaiman, Code 63Rd Department of Meteorology Naval Postgraduate School Monterey, California 93940	1
4.	Dr. C. H. Wash, Code 63Wy Department of Meteorology Naval Postgraduate School Monterey, California 93940	7
5.	LCDR Donald A. Roman, USN Box 20 Remsen, New York 13438	6
6.	Dr. Russell L. Elsberry, Code 63Es Department of Meteorology Naval Postgraduate School Monterey, California 93940	1
7.	Director Naval Oceanography Division Naval Observatory 34th and Massachusetts Avenue NW Washington, DC 20390	1
8.	Commander Naval Oceanography Command NSTL Station Bat St. Louis, MS 39522	1
9.	Dr. Scott Sandgathe, Code 63Sa Department of Meteorology Naval Posgraduate School Monterey, California 93940	1

10. Commanding Officer 1
Fleet Numerical Oceanography Center
Monterey, California 93940

11. Commanding Officer 1
Naval Ocean Research and Development Activity
NSTL Station
Bay St. Louis, MS 39522

12. Commanding Officer 1
Naval Environmental Prediction Research Activity
Monterey, California 93940

13. Chief of Naval Research 1
800 N. Quincy Street
Arlington, VA 22217

14. Office of Naval Research, Code 480 1
Naval Ocean Research and Development Activity
NSTL Station
Bay St. Louis, MS 39522

15. Scientific Liaison Office 1
Office of Naval Research
Scripps Institution of Oceanography
LaJolla, California 92037

16. Library 1
Scripps Institution of Oceanography
P. O. Box 2367
LaJolla, California 92037

17. Commander 1
Oceanographic Systems Pacific
Box 1390
Pearl Harbor, HI 96860

Thesis 195517
R68957 Roman
c.1 Application of quasi-lagrangian diagnostics and FGGE data in a study of east-coast cyclogenesis.